Earth Planets Space, **61**, 711–732, 2009

Remanence anisotropy effect on the palaeointensity results obtained from various archaeological materials, excluding pottery

Mary Kovacheva[1], Annick Chauvin[2], Neli Jordanova[1], Philippe Lanos[2,3], and Vassil Karloukovski[1,4]

[1]*Geophysical Institute, Bulgarian Academy of Sciences, Sofia, Bulgaria*
[2]*Geosciences-Rennes, UMR 6118 CNRS-University of Rennes 1, France*
[3]*IRAMAT, CNRS, UMR 5060, Université de Bordeaux 3, France*
[4]*Centre for Environmental Magnetism, Geographical Department of Lancaster University, Lancaster LA1 4YB, U.K.*

(Received December 12, 2007; Revised October 26, 2008; Accepted November 15, 2008; Online published July 27, 2009)

The effect of magnetic anisotropy on the palaeointensity results has been evaluated in different materials, including samples from archaeological structures of various ages, such as baked clay from prehistoric domestic ovens or pottery kilns, burnt soil from ancient fires, and bricks and bricks or tiles used in the kiln's construction. The remanence anisotropy was estimated by the thermoremanent (TRM) anisotropy tensor and isothermal remanence (IRM) tensor methods. The small anisotropy effect (less than 5%) observed in the palaeointensity results of baked clay from the relatively thin prehistoric oven's floors estimated previously through IRM anisotropy was confirmed by TRM anisotropy of this material. The new results demonstrate the possibility of using IRM anisotropy evaluation to correct baked clay palaeointensity data instead of the more difficult to determine TRM anisotropy ellipsoid. This is not always the case for the palaeointensity results from bricks and tiles. The anisotropy correction to palaeointensity results seems negligible for materials other than pottery. It would therefore appear that the palaeointensity determination is more sensitive to the degree of remanence anisotropy P and the angle between the natural remanent magnetization (NRM) vector and the laboratory field direction, than to the angle between the NRM and the maximum axis of the remanence anisotropy ellipsoid ($K_{\max}$).
Key words: Archaeomagnetism, baked clay materials, palaeointensity, magnetic anisotropy correction.

1. Introduction

Palaeointensity determination remains one of the most difficult tasks in palaeo- and archaeomagnetism. Palaeointensity techniques are based on a comparison between natural remanent magnetization (NRM) and an artificial magnetization given in a known laboratory field. The influence of magnetic anisotropy on the palaeointensity evaluation was suggested long time ago, and the notion of 'easy plane' was introduced, especially in the case of pottery (Rogers *et al*., 1979). To avoid the anisotropy effect Aitken *et al*. (1981) adjusted the direction of the natural remanent magnetization (NRM) of their samples as close as possible to the direction of the applied laboratory field. Veitch *et al*. (1984) suggested the determination of the thermoremanent magnetization anisotropy ellipsoids for samples of tiles and bricks. In the studies reported by Yang *et al*. (1993a, b) and Selkin *et al*. (2000), the thermoremanent anisotropy tensor was replaced by that of an induced anhysteretic remanence (ARM) tensor. Hus (2001) and Hus *et al*. (2002) showed that the partial anhysteretic remanence (pARM) anisotropy ellipsoid mimics best the TRM anisotropy ellipsoid and can be used for the correction of palaeointensity determinations. Such corrections have been applied by Yang *et al*. (1993b), Selkin *et al*. (2000) and Carvallo and Dunlop (2001). The general disadvantage to this approach is that the ARM has to be induced after the palaeointensity experiment and that the magnetic fraction carrying the ARM can be different from the one carrying the TRM due to mineralogical changes that occur during heating (Henry *et al*., 2003).

In contrast to the substantial effect of remanence anisotropy on the palaeointensity estimates from rocks with a significant petrofabric described in Selkin *et al*. (2000), Yu *et al*. (2001) reported a very weak influence of the remanence anisotropy on the palaeointensity estimates from a Tudor Gabbro, Ontario.

Garcia (1996) and Chauvin *et al*. (2000) studied the effect of anisotropy on the palaeointensity results by estimating the thermoremanent magnetization (TRM) tensor using samples from ancient bricks used in the kiln's construction. Their studies revealed that the anisotropy effect is quite important and not at all negligible reaching, in some cases, a correction factor of 25% of the determined field strength. The anisotropy effect on the palaeointensity result estimated through the anisotropy of induced isothermal remanent magnetisation (IRM), as recommended in Stephenson *et al*. (1986), has been previously performed for samples of baked clay of prehistoric ovens. This effect was found to be negligible, and the correction factor "f" of the absolute palaeointensity values is usually lower than 5% (Jordanova *et al*., 1995; Jordanova, 1996; Kovacheva *et al*., 1998). The idea of substituting the determination of the TRM anisotropy tensor by the determination of the IRM

anisotropy tensor without heating has practical advantages, but needs confirmation.

Our aim was, therefore, to compare the anisotropy correction to palaeointensity results through IRM- and TRM-induced remanence on the same material. To this end, we used archaeological samples of various origins and ages. The palaeointensity study was performed using the classical Thellier method (Thellier and Thellier, 1959) in two laboratories (the Geosciences Laboratory, University of Rennes 1, France and the Palaeomagnetic laboratory of the Geophysical Institute, Bulgarian Academy of Sciences, Sofia). In addition to other factors involved in the palaeointensity determination, such as the non-linearity of the Arai diagram, mineralogical changes, non-suitable magnetic characteristics, among others (Chauvin *et al.*, 1991; Jordanova *et al.*, 1997; Kovacheva *et al.*, 1998; Jordanova *et al.*, 2003), a detailed examination of the magnetic anisotropy effect on the palaeointensity results obtained from materials other than pottery is still required.

Here, we present multiple measurements of the magnetic anisotropy of 85 archaeomagnetic samples of different materials. Three large tables containing all of the calculated parameters of magnetic thermoremanence anisotropy measurements at different temperature steps and of the induced isothermal remanence are given.

2. Experimental Set-up

2.1 Samples

The collection of samples studied here comes from two areas (France and Bulgaria) and consists of 85 samples from baked clay floors of ovens and kilns and burnt soil of ancient fires (BC-BS), bricks as displaced material and bricks or tiles in kiln's construction (BR-TL). Bricks as displaced material presumably carry univectorial remanence. Bricks or tiles used in the construction of pottery kilns can carry a two-vector remanence when their heating as a constructive element of a kiln was not sufficient to entirely replace the primary magnetization, obtained in different position during their fabrication. Nevertheless, the effect of the shape anisotropy on the initial magnetization and that obtained during re-heating should be the same.

Samples coming from Bulgarian sites have a cubic shape with an edge of 20 mm or 24 mm. Rarely—when the quantity of archaeomagnetic material was insufficient—the cubes were completed with plaster of Paris. Samples from French sites are all of standard cylindrical shape. Bricks and tiles (BR-TL) show considerable shape anisotropy (Lanos, 1987a, b; Goulpeau *et al.*, 1989), which should affect the direction of the TRM acquired. Shape anisotropy is related to the form of the whole objects as is the case with pottery, while the anisotropy measured in the laboratory is governed by the distribution and shape of the magnetic grains. Here, we consider the effect of this latter anisotropy on the palaeointensity results, taking into account the nature of samples. It should be also mentioned that the preferential alignment of the magnetic grains carrying the remanence is in fact related to the initial form of the whole object (brick, tile, pottery), thus explaining the used term of 'easy plane'. The measured anisotropy of remanence susceptibility reflects both the shape and distribution of the magnetic grains due to the object's form. 'Easy plane' in archaeological objects corresponds to the petrofabric in rocks.

2.2 Methodology

Remanent magnetization was measured at Rennes with a Molspin spinner magnetometer and in Sofia with an astatic magnetometer. The classical Thellier method (Thellier and Thellier, 1959) for palaeointensity determination consists of a double heating of samples, with each temperature step performed in applied laboratory magnetic field. The re-magnetization is made successively to higher temperatures, with several partial thermoremanence acquisition (pTRM) tests (Coe *et al.*, 1978). The direction of the TRM acquired during natural (initial) cooling by objects with shape anisotropy or petrofabric deviates from the local direction of the geomagnetic field, and the intensity of the TRM depends on the direction in which the local field is applied. During the course of the Thellier experiments, the TRM anisotropy should be taken into account if the samples are not re-magnetized in the direction of their initial TRM (Odah *et al.*, 2001). Because of the fact that this condition is rarely met in the usual practice, we aim to quantitatively evaluate the possible errors for materials different from potteries.

The anisotropy effect on the palaeointensity result has been studied both using the TRM anisotropy evaluation, performed twice for most of the samples, and the IRM anisotropy evaluation on the same samples, performed after the Thellier experiment (in the laboratories in both Sofia and Rennes). Both a Schonstedt static AF demagnetizer (in Rennes) and a thumbling Molspin AF demagnetizer (in Sofia) were used.

2.3 TRM anisotropy determination

The determination of the TRM anisotropy tensor was done first alongside the usual procedure of the Thellier experiment at temperatures corresponding to known major unblocking temperatures of NRM. To ensure that the new remanence was obtained by the un-altered assemblage of magnetic grains, these temperatures were taken between 430 and 450°C if positive (pTRM) tests were observed. In order to evaluate the TRM anisotropy, we performed five additional heatings at the chosen temperature step at which the samples had already been re-magnetized along their $\pm Z$ axes. The additional four re-magnetizations were along the $\pm X$ and $\pm Y$ axes. Finally, a last re-magnetization was performed along the $+Z$ axis of the samples in order to check their thermal stability. If no or few modifications of the TRM acquisition capacity were observed, the TRM anisotropy tensor was then determined (Chauvin *et al.*, 2000), otherwise the sample was rejected. Due to the fact that the first determination of thermoremanent anisotropy (TRM1) was evaluated during several palaeointensity batches/runs of BC-BS and BR-TL samples, the temperature of this evaluation differed for different batches, and this is noted accordingly in tables and figures. At the end of the Thellier experiment (temperature of 550 or 620°C), when almost all the original NRM was removed, the thermoremanent anisotropy tensor (TRM2) was evaluated once again.

Anisotropy parameters describing the TRM tensor were calculated (the principal axes denoted as $K_{\max}$, K_{int}, and

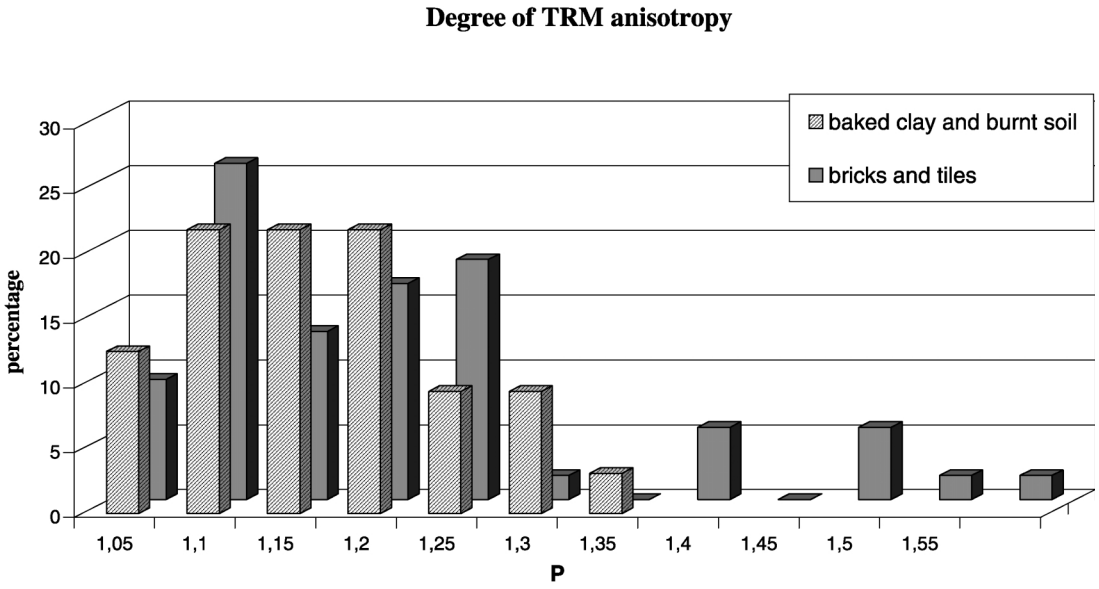

Fig. 1. Histogram showing the frequency distribution in percentage of the measured TRM1 degree of anisotropy, obtained by the samples from baked clay/burnt soils (BC-BS) and the same for bricks/tiles (BR-TL) samples.

$K_{\min}$), as were their orientations in sample co-ordinates. The anisotropy parameters consisted of: lineation ($L = K_{\max}/K_{\text{int}}$), foliation ($F = K_{\text{int}}/K_{\min}$), the shape parameter ($T = (2\eta_2 - \eta_1 - \eta_3)/(\eta_1 - \eta_3)$, where $\eta_1 = \ln K_{\max}$, $\eta_2 = \ln K_{\text{int}}$, $\eta_3 = \ln K_{\min}$), and the degree of anisotropy ($P = K_{\max}/K_{\min}$) (Jelinek, 1981; Hrouda, 1982; Stephenson *et al.*, 1986). Both vectors (NRM remained and pTRM gained) were corrected at each temperature step of the Thellier experiment. Thus, the corrected Arai diagram (Nagata *et al.*, 1963) and the corrected palaeointensity value (H_{acor}) were obtained. The correction factor f is the ratio $H_{\text{acor}}/H_{\text{a}}$, where H_{a} is the palaeointensity value without correction for remanence anisotropy. f can also be expressed as the percentage difference from the non-corrected palaeointensity value (thus $f = 1.04$ corresponds to a 4% difference of the H_{acor} from H_{a}).

2.4 IRM anisotropy determination

The anisotropy of IRM was calculated on the same samples as those used in the Thellier experiment, after the last heating step. A steady magnetic field of 60 mT was applied, inducing IRM successively along $\pm X$, $\pm Y$, and $\pm Z$ axes of the specimen. While working with archaeological materials, Marton (1996) mentioned that if a low steady field is used, the IRM ellipsoid should be dominated by multidomain (MD) particles. Thus, an intensity of 50–60 mT is necessary (Stephenson *et al.*, 1986; Tarling and Hrouda, 1993, p. 81) to ensure that the anisotropy ellipsoid is determined on the single domain (SD) particles, which carry almost all of the NRM. At the same time, the field should not be higher in order to remain at the so-called region of Rayleigh where the IRM is proportional to the square of the applied field (Daly and Zinsser, 1973). Between the successive magnetizations, the samples are demagnetized by an alternating field (AF) of 100 mT. The residual magnetization observed after AF demagnetization appears to be negligible compared to the intensity of the IRM acquired, which is consistent with the prevailing low magnetic coercivity of our samples (MDF being in the range of 15–25 mT for most of them).

Following the proposal of Veitch *et al.* (1984), we defined a unit vector $\boldsymbol{h}$ of the ancient magnetic field by:

$$\boldsymbol{h} = (K_{\text{I}})^{-1}.\mathbf{NRM}/|(K_{\text{I}})^{-1}.\mathbf{NRM}|,$$

where $(K_{\text{I}})^{-1}$ is the inverse anisotropy tensor of the laboratory-induced IRM.

Then, the correction factor f is the ratio of IRM acquired by the unit field parallel to the direction of the known laboratory field during the experiment and IRM acquired by the unit field parallel to $\boldsymbol{h}$. Or:

$$f = |(K_{\text{I}}) \cdot \boldsymbol{l}| \,/\, |(K_{\text{I}}) \cdot \boldsymbol{h}|$$

where $\boldsymbol{l}$ is the unit vector along the laboratory field.

Principal axes of the corresponding IRM tensors and anisotropy parameters are denoted the same as those for the TRM anisotropy, defined above.

3. Experimental Results

Taking into account the different nature of the studied samples, the results are given separately for baked clay/burnt soils (BC-BS) and for bricks/tiles (BR-TL). The relationship between the anisotropy parameters obtained at different temperature steps during the palaeointensity experiment (TRM1 and TRM2) and between parameters obtained by the thermoremanent anisotropy ellipsoid and the IRM one is considered.

3.1 TRM anisotropy evaluation at two temperatures

The degree of TRM1 anisotropy (P) of 33 BC-BS samples measured at an intermediate temperature (428 or 450°C) is relatively weak (Fig. 1). Of the samples studied, 12% have $P \leq 1.05$ and 67% have $1.05 < P \leq 1.2$. There is only one case with $P = 1.31$. The degree of TRM1 anisotropy for 52 BR-TL samples (at 440 or 450°C) is higher than that for the BC-BS samples (Fig. 1). We have

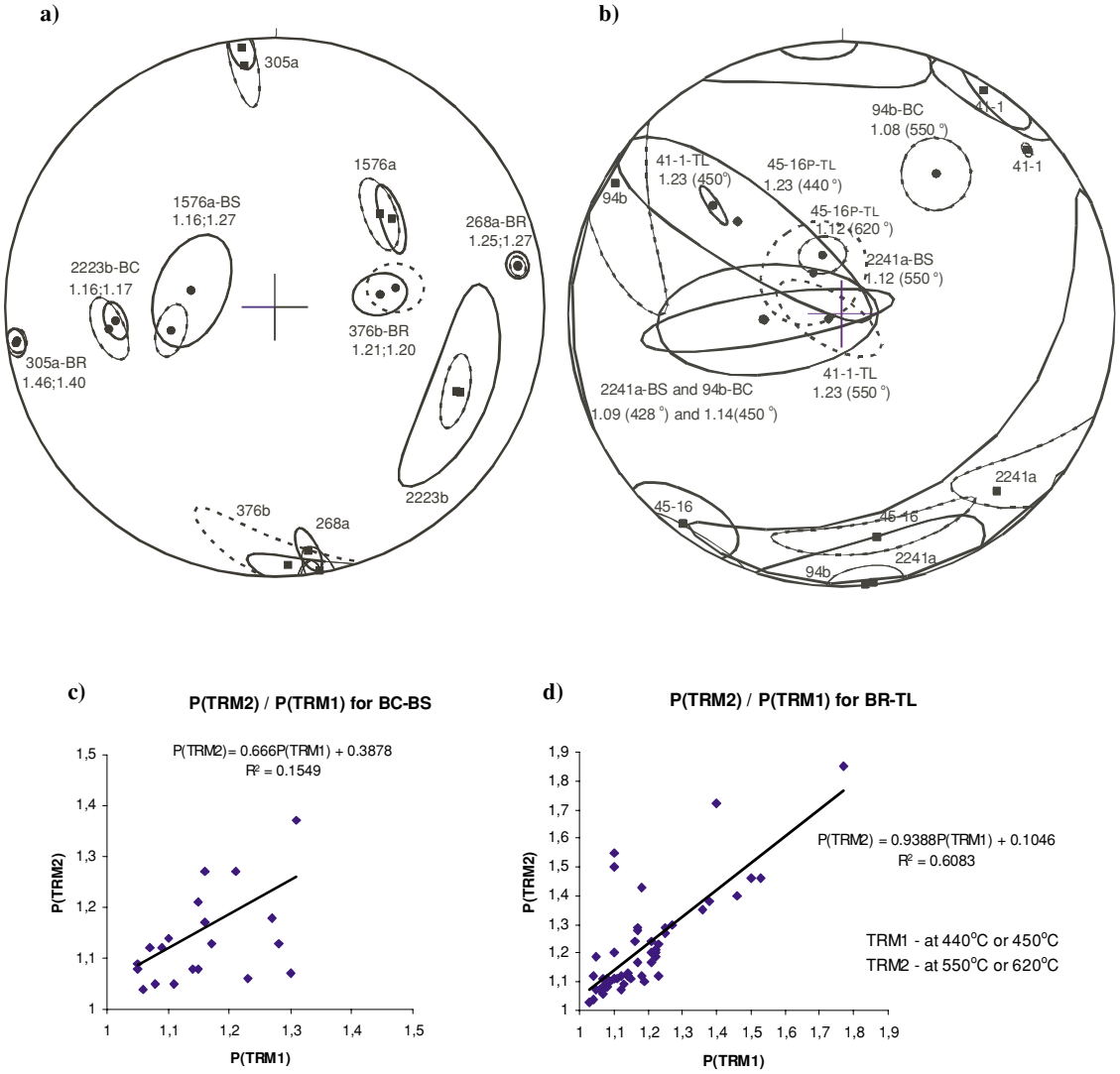

Fig. 2. Stereographic projections, in sample co-ordinates, of the principal maximal and minimal axes' directions of the TRM ellipsoids determined at two different temperatures for some typical samples; dots denote the minimal axes and squares denoted the maximal axes. (a) a good consistency; (b) bad consistency of the principal axes directions. The sample numbers and the type of material are shown together with the degree of remanence anisotropy at the two temperature levels (the second line). The stereographic projections are given in the lower hemisphere, with the confidence ellipses given with dashed lines for the higher temperature evaluation (TRM2); (c) and (d) relationships between the remanence degree of anisotropy P at the two temperature levels for different type of materials.

fewer than 10% of cases with $P \leq 1.05$ and 56% in which $1.05 < P \leq 1.2$, but in 32% of cases $1.2 < P \leq 1.5$. In two cases, P exceeds this upper limit (samples 34-15P and 1596v with a highest value of 1.77; Table 2). A total of 158 TRM anisotropy evaluations were made on the 85 samples.

One basic condition for a comparison of anisotropy tensors obtained at two different temperatures is that the same assemblages of magnetic carriers participate in the two evaluations.

In the BC-BS materials, some external factors, such as irregularities in the cube's shape, can influence the measured weaker anisotropy parameters; four prehistoric samples have been excluded because of their imperfect shape. A series of BC-BS and BR-TL samples has been subjected to a second evaluation of the anisotropy tensor at a higher temperature (TRM2 at 550°C), using a different sample holder, allowing for a better positioning of the samples within the oven. Additionally, 27 BR-TL samples were studied for their TRM anisotropy twice (at 440°C and 620°C; Table 2, lower part), with a very precise positioning in a specially designed holder. The coincidence of the directions of the principal remanence anisotropy axes, evaluated at two different temperature steps, is good in many cases (Fig. 2(a); samples 1576a and 2223b). For samples with stronger anisotropy degree like BR-TL, these directions are determined more precisely (Fig. 2(a); samples 305a, 376b, 268a) despite the probability of a bad positioning at the lower temperature. Samples with weaker anisotropy, however, show a very large uncertainty in terms of the directions of the principal axes (Fig. 2(b); samples 2241a, 94b). A closer look at Fig. 2(b) shows that, in most cases, the principal directions determined at the lower temperature have unacceptably large errors and cannot be considered to be real. This fact probably partly reflects the bad positioning of some samples, mentioned above using the first holder for the TRM1 anisotropy measurements at the lower tempera-

Table 1. TRM anisotropy parameters obtained for samples of baked clay and burnt soil (BC-BS) at two temperatures: during the Thellier palaeointensity experiment (428° or 450°C) and at the end of the same experiment (550°C); IRM anisotropy parameters obtained after the palaeointensity experiment by a steady field of 60 mT. The shape parameters T are given below the foliation (F) parameter in each case.

	ANISOTROPY OF TRM1						ANISOTROPY OF TRM2						ANISOTROPY OF IRM					
No	428 (deg. C)			L	F	P	550 (deg. C)			L	F	P	(60 mT)			L	F	P
material		D	I	K1/K2	K2/K3	K1/K3		D	I	K1/K2	K2/K3	K1/K3		D	I	K1/K2	K2/K3	K1/K3
I 11b	K1	260	44	1,06	1,08	1,15	K1	55	26	1,02	1,06	1,08	K1	78	42	1,05	1,01	1,06
baked	K2	4	15		T		K2	318	13		T		K2	252	47		T	
clay	K3	109	43		0,15		K3	204	61		0,57		K3	345	2		-0,72	
I 9v	K1	238	46	1,03	1,06	1,10							K1	223	63	1,04	1,01	1,05
baked	K2	136	11		T								K2	322	4		T	
clay	K3	36	42		0,28								K3	55	26		-0,78	
CA54a	K1	156	2	1,02	1,28	1,31	K1	43	1	1,01	1,36	1,37	K1	241	24	1,09	1,02	1,11
baked	K2	246	11		T		K2	313	1		T		K2	138	26		T	
clay	K3	57	79		0,88		K3	178	88		0,94		K3	8	52		-0,90	
D174g	K1	152	19	1,07	1,07	1,15	K1	134	24	1,04	1,16	1,21	K1	152	62	1,01	1,04	1,05
baked	K2	57	15		T		K2	39	13		T		K2	270	13		T	
clay	K3	290	66		0,01		K3	283	63		0,57		K3	5	23		0,68	
D192v	K1	65	14	1,02	1,06	1,08							K1	0	46	1,05	1,04	1,09
baked	K2	155	0		T								K2	117	23		T	
clay	K3	242	76		0,49								K3	224	34		-0,08	
Hd	K1	204	46	1,02	1,09	1,10	K1	357	45	1,07	1,06	1,14	K1	276	67	1,06	1,10	1,16
burnt	K2	26	44		T		K2	123	30		T		K2	155	11		T	
soil	K3	295	1		0,67		K3	233	29		-0,10		K3	61	18		0,22	
2073a	K1	261	43	1,13	1,16	1,30	K1	260	15	1,01	1,06	1,07	K1	233	26	1,03	1,01	1,04
burnt	K2	353	2		T		K2	357	24		T		K2	332	18		T	
soil	K3	85	47		0,10		K3	141	61		0,71		K3	93	57		-0,69	
2085v	K1	79	51	1,11	1,15	1,28	K1	54	4	1,06	1,06	1,13	K1	209	37	1,02	1,09	1,11
burnt	K2	195	20		T		K2	152	63		T		K2	87	34		T	
soil	K3	299	32		0,14		K3	323	27		-0,07		K3	330	33		0,62	
2085g	K1	112	64	1,09	1,06	1,16							K1	178	38	1,03	1,12	1,16
burnt	K2	224	10		T								K2	56	34		T	
soil	K3	313	24		-0,18								K3	300	33		0,60	
2168a	K1	108	32	1,01	1,16	1,17	K1	104	9	1,05	1,08	1,13	K1	165	54	1,01	1,09	1,10
burnt	K2	214	24		T		K2	202	38		T		K2	262	4		T	
soil	K3	334	48		0,90		K3	3	51		0,25		K3	355	35		0,83	
2192a	K1	31	60	1,03	1,08	1,11							K1	106	60	1,04	1,08	1,12
baked	K2	210	30		T								K2	239	21		T	
clay	K3	300	0		0,43								K3	337	20		0,29	
2192b	K1	351	75	1,04	1,16	1,20							K1	197	1	1,06	1,05	1,12
baked	K2	163	15		T								K2	288	33		T	
clay	K3	254	2		0,61								K3	105	56		-0,10	
DG23e	K1	212	13	1,02	1,03	1,05	K1	296	28	1,01	1,07	1,08	K1	67	12	1,02	1,05	1,08
baked	K2	315	45		T		K2	31	9		T		K2	303	69		T	
clay	K3	110	42		0,20		K3	138	60		0,79		K3	161	16		0,39	
DG37d	K1	140	19	1,10	1,04	1,14							K1	327	42	1,07	1,02	1,09
baked	K2	33	41		T								K2	104	39		T	
clay	K3	248	43		-0,41								K3	215	23		-0,55	
DG45d	K1	110	28	1,03	1,08	1,12							K1	131	41	1,02	1,05	1,07
baked	K2	1	31		T								K2	25	18		T	
clay	K3	233	46		0,49								K3	276	43		0,40	
2241a	K1	173	1	1,05	1,04	1,09	K1	139	15	1,01	1,11	1,12	K1	119	6	1,04	1,11	1,16
burnt	K2	83	23		T		K2	229	2		T		K2	25	33		T	
soil	K3	266	67		-0,08		K3	326	75		0,75		K3	219	56		0,42	
2242a	K1	54	22	1,04	1,16	1,21	K1	91	38	1,15	1,43	1,65	K1	88	14	1,12	1,04	1,16
burnt	K2	150	15		T		K2	181	1		T		K2	191	40		T	
soil	K3	272	63		0,56		K3	272	52		0,44		K3	343	45		-0,50	

ture.

The fact that sample 45-16P from the group of 27 BR-TL for which the two evaluations are made using a good holder has given a bad comparison of the directions of the principal axes (Fig. 2(b)) shows the prevailing effect of the insufficient determinism of the tensor through three perpendicular measurements than that of the holder not permitting a very precise positioning. Moreover, the P of this sample is not as high (1.23 at 440°C and 1.12 at 620°C). Samples with a weaker degree of anisotropy do not give satisfactory results

Table 1. (continued).

No material	ANISOTROPY OF TRM1						ANISOTROPY OF TRM2						ANISOTROPY OF IRM					
	428 (deg. C)			L	F	P	550 (deg. C)			L	F	P	(60 mT)			L	F	P
		D	I	K1/K2	K2/K3	K1/K3		D	I	K1/K2	K2/K3	K1/K3		D	I	K1/K2	K2/K3	K1/K3
2253a	K1	131	3	1,03	1,06	1,10							K1	319	11	1,03	1,06	1,09
burnt	K2	41	13		T								K2	227	6		T	
soil	K3	232	77		0,28								K3	109	76		0,33	
2264v	K1	241	24	1,05	1,16	1,21	K1	132	8	1,12	1,13	1,27	K1	57	15	1,08	1,10	1,18
burnt	K2	147	8		T		K2	40	10		T		K2	321	20		T	
soil	K3	41	65		0,53		K3	261	77		0,02		K3	181	63		0,20	
GV33b	K1	179	0	1,02	1,03	1,05							K1	188	44	1,03	1,07	1,10
baked	K2	89	33		T								K2	73	23		T	
clay	K3	270	57		0,13								K3	324	36		0,46	
GV45v	K1	124	40	1,02	1,21	1,23	K1	352	11	1,03	1,03	1,06	K1	261	28	1,05	1,03	1,08
burnt	K2	24	12		T		K2	92	42		T		K2	131	50		T	
soil	K3	280	48		0,80		K3	251	46		0,08		K3	6	25		-0,25	
2145b	K1	126	44	1,11	1,07	1,19							K1	336	30	1,01	1,06	1,07
burnt	K2	35	2		T								K2	86	30		T	
soil	K3	303	46		-0,16								K3	211	43		0,80	
2215b	K1	218	0	1,00	1,01	1,01							K1	133	58	1,01	1,08	1,10
baked	K2	128	9		T								K2	254	17		T	
clay	K3	322	81		0,86								K3	353	25		0,69	
2221b	K1	237	44	1,08	1,03	1,12							K1	256	2	1,05	1,01	1,06
baked	K2	357	28		T								K2	346	2		T	
clay	K3	107	33		-0,41								K3	123	87		-0,55	
No material	ANISOTROPY OF TRM1						ANISOTROPY OF TRM2						ANISOTROPY OF IRM					
	450 (deg. C)			L	F	P	550 (deg. C)			L	F	P	(60 mT)			L	F	P
		D	I	K1/K2	K2/K3	K1/K3		D	I	K1/K2	K2/K3	K1/K3		D	I	K1/K2	K2/K3	K1/K3
101v	K1	57	29	1,03	1,05	1,08	K1	54	6	1,02	1,03	1,05	K1	249	0	1,01	1,02	1,04
baked	K2	273	56		T		K2	312	62		T		K2	339	65		T	
clay	K3	157	17		0,24		K3	147	27		0,02		K3	159	24		0,30	
641a	K1	79	39	1,04	1,06	1,11	K1	303	49	1,03	1,01	1,05	K1	269	6	1,03	1,02	1,05
burnt	K2	280	48		T		K2	57	20		T		K2	15	66		T	
soil	K3	178	11		0,17		K3	162	34		-0,52		K3	177	22		-0,11	
642b	K1	44	8	1,02	1,05	1,07	K1	243	15	1,02	1,10	1,12	K1	1	64	1,06	1,12	1,18
burnt	K2	303	51		T		K2	1	60		T		K2	237	13		T	
soil	K3	141	38		0,45		K3	146	26		0,72		K3	142	20		0,34	
94b	K1	175	1	1,11	1,02	1,14	K1	300	5	1,02	1,06	1,08	K1	99	21	1,01	1,05	1,06
baked	K2	85	23		T		K2	204	52		T		K2	229	58		T	
clay	K3	266	67		-0,65		K3	34	38		0,59		K3	0	21		0,69	
1509a	K1	267	9	1,01	1,04	1,05	K1	348	4	1,06	1,03	1,09	K1	16	40	1,03	1,01	1,04
burnt	K2	18	67		T		K2	255	39		T		K2	112	7		T	
soil	K3	173	21		0,73		K3	83	51		-0,32		K3	211	49		-0,39	
1788a	K1	100	1	1,03	1,23	1,27	K1	113	3	1,01	1,17	1,18	K1	89	0	1,02	1,14	1,16
baked	K2	10	3		T		K2	204	0		T		K2	359	0		T	
clay	K3	210	87		0,76		K3	301	87		0,91		K3	214	89		0,74	
86v	K1	101	4	1,03	1,03	1,06	K1	117	8	1,02	1,02	1,04	K1	278	7	1,01	1,02	1,03
baked	K2	192	11		T		K2	26	8		T		K2	187	10		T	
clay	K3	350	78		0,03		K3	249	79		0,03		K3	43	77		0,20	
2223b	K1	115	25	1,05	1,10	1,16	K1	115	27	1,07	1,09	1,17	K1	3	5	1,03	1,00	1,04
baked	K2	22	5		T		K2	16	17		T		K2	135	82		T	
clay	K3	281	64		0,28		K3	257	58		0,15		K3	272	5		0,77	
1576a	K1	53	45	1,05	1,12	1,16	K1	48	47	1,11	1,14	1,27	K1	55	58	1,17	1,10	1,29
burnt	K2	160	17		T		K2	158	18		T		K2	167	12		T	
soil	K3	265	40		0,34		K3	263	38		0,14		K3	263	28		-0,25	

on the directions of the principal axes of the TRM ellipsoid and, thus, the tensors' orientations cannot be compared reliably. Therefore, it should be noted that for the purposes of any anisotropy correction of the palaeointensity results, the tensor determination by measurements on three perpendicular directions, as done here, is sufficient—but probably not sufficient for determination of the directions of the principal axes, especially for samples with a weak anisotropy.

The BC-BS samples do not show a good consistency among the values of anisotropy parameters (Fig. 2(c); Table 1). The degree of TRM anisotropy at two different temperature levels for the BR-TL samples is similar, as shown in Garcia (1996) and Chauvin *et al.* (2000), although there are some outliers here (Fig. 2(d); Table 2). The sim-

Table 2. The same as in Table 1 but for samples from bricks and tiles (BR-TL). The lower temperature is 440° or 450°C and the higher temperature, 550°C or 620°C.

No		ANISOTROPY OF TRM1						ANISOTROPY OF TRM2						ANISOTROPY OF IRM					
material		450 (deg. C)		L	F	P		550 (deg. C)		L	F	P		(60 mT)		L	F	P	
		D	I	K1/K2	K2/K3	K1/K3		D	I	K1/K2	K2/K3	K1/K3		D	I	K1/K2	K2/K3	K1/K3	
69b	K1	353	46	1.05	1.03	1.08	K1	331	63	1.04	1.06	1.11	K1	333	41	1.03	1.02	1.05	
brick	K2	223	31		T		K2	207	15		T		K2	243	0		T		
	K3	115	27		-0.33		K3	111	21		0.20		K3	152	48		-0.26		
268a	K1	170	1	1.06	1.18	1.25	K1	172	10	1.06	1.2	1.27	K1	344	7	1.05	1.11	1.16	
brick	K2	266	80		T		K2	307	76		T		K2	207	79		T		
	K3	80	10		0.45		K3	80	10		0.54		K3	75	7		0.38		
269a	K1	171	50	1.08	1.27	1.38	K1	174	54	1.07	1.29	1.38	K1	163	77	1.12	1.14	1.28	
brick	K2	0	39		T		K2	359	36		T		K2	2	12		T		
	K3	266	5		0.49		K3	267	3		0.58		K3	271	4		0.12		
302v	K1	6	9	1.05	1.18	1.25	K1	5	11	1.08	1.19	1.29	K1	5	14	1.03	1.13	1.17	
brick	K2	249	70		T		K2	245	68		T		K2	248	61		T		
	K3	99	18		0.42		K3	98	19		0.41		K3	102	24		0.60		
376b	K1	170	2	1.06	1.14	1.21	K1	177	5	1.04	1.15	1.20	K1	248	38	1.01	1.12	1.14	
brick	K2	259	32		T		K2	271	37		T		K2	341	3		T		
	K3	83	58		0.42		K3	81	53		0.56		K3	76	51		0.83		
1609a	K1	112	40	1.09	1.05	1.14	K1	141	46	1.07	1.06	1.13	K1	110	62	1.11	1.08	1.20	
brick	K2	221	21		T		K2	236	4		T		K2	229	14		T		
	K3	332	42		-0.32		K3	330	44		-0.12		K3	325	24		-0.15		
70b	K1	198	10	1.06	1.03	1.09	K1	204	4	1.05	1.04	1.10	K1	216	17	1.06	1.04	1.10	
brick	K2	297	44		T		K2	300	52		T		K2	346	63		T		
	K3	98	45		-0.25		K3	111	37		-0.15		K3	119	18		-0.19		
270a	K1	188	7	1.06	1.16	1.22	K1	11	3	1.04	1.17	1.21	K1	46	51	1.01	1.11	1.12	
brick	K2	75	74		T		K2	110	70		T		K2	185	31		T		
	K3	280	15		0.44		K3	280	19		0.62		K3	288	21		0.83		
305a	K1	353	3	1.10	1.32	1.46	K1	353	10	1.06	1.33	1.40	K1	349	17	1.04	1.15	1.20	
brick	K2	120	85		T		K2	154	79		T		K2	142	70		T		
	K3	263	4		0.47		K3	262	3		0.67		K3	256	8		0.55		
379a	K1	285	60	1.03	1.04	1.06	K1	299	63	1.02	1.05	1.07	K1	11	48	1.02	1.03	1.06	
brick	K2	189	3		T		K2	196	6		T		K2	226	36		T		
	K3	98	30		0.17		K3	102	26		0.27		K3	122	17		0.28		
551b	K1	39	2	1.04	1.03	1.07	K1	216	6	1.02	1.04	1.07	K1	236	1	1.03	1.02	1.05	
brick	K2	129	13		T		K2	126	1		T		K2	326	7		T		
in constr.	K3	299	77		-0.08		K3	30	84		0.33		K3	138	83		-0.26		
					T														
36-3	K1	274	68	1.06	1.05	1.11	K1	227	22	1.04	1.06	1.11	K1	249	54	1.04	1.02	1.06	
tile	K2	47	15		T		K2	347	51		T		K2	123	22		T		
in constr.	K3	141	15		-0.06		K3	124	30		0.20		K3	21	25		-0.39		
36-8	K1	294	19	1.03	1.09	1.12	K1	61	18	1.05	1.07	1.12	K1	85	45	1.07	1.08	1.15	
tile	K2	42	41		T		K2	323	22		T		K2	306	37		T		
in constr.	K3	186	43		0.52		K3	187	61		0.19		K3	198	22		0.10		
36-13	K1	14	29	1.07	1.09	1.17	K1	2	21	1.02	1.14	1.17	K1	301	32	1.02	1.07	1.10	
tile	K2	107	6		T		K2	269	6		T		K2	44	19		T		
in constr.	K3	207	61		0.11		K3	163	68		0.72		K3	159	50		0.52		
36-16	K1	222	9	1.08	1.08	1.17	K1	48	2	1.21	1.07	1.29	K1	63	7	1.02	1.02	1.05	
tile	K2	319	40		T		K2	302	81		T		K2	331	12		T		
in constr.	K3	121	49		0.02		K3	138	9		-0.46		K3	182	76		-0.01		
36-17	K1	210	11	1.03	1.01	1.04	K1	232	1	1.08	1.04	1.12	K1	257	9	1.02	1.07	1.09	
tile	K2	114	29		T		K2	322	10		T		K2	163	21		T		
in consrt.	K3	318	59		-0.61		K3	134	80		-0.36		K3	9	66		0.39		

ple recalculation of the regression line without these outliers gives a similar regression equation: $P(\mathrm{TRM2}) = 0.9386P(\mathrm{TRM1}) + 0.0778$, with a significantly better regression coefficient ($R^2 = 0.8776$) as should be expected, but pointing that their influence is not as important.

Nevertheless, we have strong proof that the anisotropy evaluations at two temperatures are in general identical—as is shown in Fig. 3, where the relationship between the

Table 2. (continued).

No		ANISOTROPY OF TRM1						ANISOTROPY OF TRM2						ANISOTROPY OF IRM				
material		450 (deg. C)		L	F	P		550 (deg. C)		L	F	P		(60 mT)		L	F	P
		D	I	K1/K2	K2/K3	K1/K3		D	I	K1/K2	K2/K3	K1/K3		D	I	K1/K2	K2/K3	K1/K3
36-19	K1	153	9	1.07	1.03	1.10	K1	135	14	1.08	1.02	1.11	K1	114	9	1.02	1.03	1.04
tile	K2	289	78		T		K2	35	35		T		K2	268	79		T	
in constr.	K3	61	8		-0.40		K3	243	51		-0.54		K3	24	4		0.25	
41-1	K1	48	10	1.18	1.05	1.23	K1	32	3	1.13	1.10	1.23	K1	294	1	1.14	1.06	1.20
tile	K2	151	50		T		K2	122	2		T		K2	31	85		T	
in constr.	K3	310	38		-0.57		K3	250	86		-0.13		K3	204	5		-0.37	
41-4	K1	52	12	1.07	1.08	1.16	K1	155	3	1.13	1.10	1.24	K1	102	7	1.02	1.11	1.14
tile	K2	146	17		T		K2	64	7		T		K2	193	7		T	
in constr.	K3	288	69		0.04		K3	272	83		-0.16		K3	329	79		0.75	
41-6	K1	53	2	1.05	1.09	1.14	K1	160	8	1.08	1.04	1.12	K1	247	1	1.01	1.04	1.04
tile	K2	151	79		T		K2	252	45		T		K2	337	0		T	
in constr.	K3	322	11		0.24		K3	36	75		-0.34		K3	85	88		0.70	
41-8	K1	225	16	1.11	1.06	1.18	K1	89	1	1.06	1.05	1.12	K1	240	37	1.01	1.01	1.02
tile	K2	48	74		T		K2	181	62		T		K2	51	52		T	
in constr.	K3	315	1		-0.26		K3	91	0		-0.05		K3	147	4		0.17	
41-9	K1	157	0	1.07	1.14	1.22	K1	33	8	1.09	1.10	1.19	K1	53	13	1.02	1.07	1.09
tile	K2	67	2		T		K2	124	3		T		K2	320	10		T	
in constr.	K3	257	88		0.28		K3	235	81		0.04		K3	193	73		0.50	
41-19	K1	25	30	1.10	1.04	1.15	K1	304	13	1.05	1.05	1.10	K1	251	11	1.02	1.04	1.06
tile	K2	258	47		T		K2	36	9		T		K2	348	29		T	
in constr.	K3	133	28		-0.36		K3	159	74		-0.06		K3	143	57		0.38	

No		ANISOTROPY OF TRM1						ANISOTROPY OF TRM2				
material		440 (deg. C)		L	F	P		620 (deg. C)		L	F	P
		D	I	K1/K2	K2/K3	K1/K3		D	I	K1/K2	K2/K3	K1/K3
41-6a	K1	86	11	1.01	1.07	1.08	K1	110	15	1.00	1.10	1.10
tile	K2	179	14		T		K2	202	6		T	
in constr.	K3	319	72		0.73		K3	313	74		0.92	
41-19a	K1	215	8	1.03	1.03	1.07	K1	327	13	1.07	1.04	1.11
tile	K2	315	52		T		K2	236	6		T	
in constr.	K3	119	37		-0.06		K3	121	76		-0.24	
B175b	K1	207	50	1.02	1.01	1.03	K1	196	20	1.02	1.01	1.03
brick	K2	6	38		T		K2	98	25		T	
	K3	104	11		-0.21		K3	323	57		-0.47	
B178a	K1	193	29	1.06	1.07	1.13	K1	180	27	1.04	1.05	1.09
brick	K2	84	30		T		K2	72	32		T	
	K3	318	46		0.10		K3	302	46		0.03	
B182b	K1	184	62	1.06	1.05	1.12	K1	313	61	1.03	1.05	1.07
brick	K2	338	26		T		K2	177	22		T	
	K3	73	11		-0.07		K3	79	18		0.27	
B207b	K1	153	20	1.05	1.02	1.07	K1	157	25	1.05	1.00	1.06
brick	K2	60	9		T		K2	264	32		T	
	K3	307	68		-0.33		K3	37	47		-0.94	
B210a	K1	248	58	1.03	1.04	1.07	K1	250	64	1.05	1.03	1.08
brick	K2	359	12		T		K2	9	13		T	
	K3	95	28		0.12		K3	104	22		-0.28	
B211a	K1	329	3	1.02	1.02	1.04	K1	205	3	1.00	1.04	1.04
brick	K2	233	59		T		K2	256	76		T	
	K3	61	31		0.08		K3	64	14		0.90	

normalized principal values of TRM1 and TRM2 ellipsoids (normalization made by their average) for all samples subjected to two evaluations is given. In the case when a specially designed holder was used for the two evaluations (Fig. 3(b)), the linear relation is clearly close to 1, pointing to the origin of the system of co-ordinates and thus proving the identical shape of the anisotropy ellipsoids (Stephenson, 1986; Hus *et al.*, 2002). The results of samples for which a

Table 2. (continued).

No material		ANISOTROPY OF TRM1 440 (deg. C) D	I	L K1/K2	F K2/K3	P K1/K3		ANISOTROPY OF TRM2 620 (deg. C) D	I	L K1/K2	F K2/K3	P K1/K3
552a	K1	40	16	1.03	1.05	1.08	K1	51	25	1.02	1.06	1.08
brick	K2	208	73		T		K2	220	65		T	
in constr.	K3	309	3		0.27		K3	319	4		0.49	
1596v	K1	193	65	1.17	1.51	1.77	K1	192	64	1.15	1.61	1.85
brick	K2	342	22		T		K2	340	22		T	
	K3	77	11		0.45		K3	75	12		0.55	
36-19a	K1	322	45	1.07	1.03	1.10	K1	293	15	1.08	1.11	1.20
tile	K2	172	41		T		K2	200	9		T	
in constr.	K3	68	15		-0.44		K3	80	73		0.16	
45-8P	K1	87	12	1.00	1.10	1.10	K1	129	2	1.16	1.33	1.55
tile	K2	277	78		T		K2	246	87		T	
in constr.	K3	177	2		0.92		K3	39	3		0.31	
45-12P	K1	40	2	1.10	1.04	1.14	K1	41	0	1.09	1.03	1.12
tile	K2	136	69		T		K2	132	50		T	
in constr.	K3	310	20		-0.46		K3	341	40		-0.51	
45-15P	K1	33	4	1.08	1.10	1.19	K1	330	11	1.05	1.05	1.10
tile	K2	256	85		T		K2	157	78		T	
in constr.	K3	123	3		0.15		K3	60	1		-0.05	
45-16P	K1	217	4	1.17	1.05	1.23	K1	171	18	1.02	1.09	1.12
tile	K2	124	42		T		K2	80	3		T	
in constr.	K3	311	48		-0.54		K3	342	72		0.60	
45-17P	K1	126	2	1.10	1.11	1.22	K1	152	14	1.10	1.09	1.20
tile	K2	211	64		T		K2	261	52		T	
in constr.	K3	36	27		0.01		K3	53	34		-0.07	
45-18P	K1	131	40	1.03	1.17	1.21	K1	133	31	1.07	1.18	1.24
tile	K2	287	47		T		K2	285	56		T	
in constr.	K3	31	12		0.65		K3	35	13		0.45	
45-19P	K1	112	7	1.02	1.03	1.05	K1	220	6	1.02	1.05	1.07
tile	K2	209	43		T		K2	315	40		T	
in constr.	K3	15	46		0.09		K3	123	49		0.32	
45-20P	K1	158	9	1.05	1.01	1.05	K1	138	10	1.13	1.05	1.19
tile	K2	21	78		T		K2	3	76		T	
in constr.	K3	250	8		-0.75		K3	230	10		-0.41	
45-21P	K1	115	21	1.10	1.16	1.27	K1	114	24	1.11	1.17	1.30
tile	K2	1	47		T		K2	357	46		T	
in constr.	K3	221	35		0.21		K3	222	34		0.21	
45-22P	K1	300	11	1.08	1.08	1.17	K1	316	6	1.23	1.04	1.28
tile	K2	34	17		T		K2	68	73		T	
in constr.	K3	178	69		0.04		K3	224	15		-0.66	
45-23P	K1	26	21	1.04	1.06	1.10	K1	201	2	1.07	1.40	1.50
tile	K2	270	48		T		K2	314	84		T	
in constr.	K3	131	34		0.22		K3	111	5		0.67	
45-24P	K1	136	12	1.03	1.07	1.10	K1	137	3	1.02	1.09	1.11
tile	K2	238	42		T		K2	330	48		T	
in constr.	K3	34	45		0.43		K3	44	42		0.75	
45-25P	K1	43	5	1.23	1.11	1.36	K1	46	4	1.29	1.05	1.35
tile	K2	157	78		T		K2	212	72		T	
in constr.	K3	312	11		-0.34		K3	314	17		-0.66	

doubt exists on the positioning at lower temperatures show a slope quite close to 1 but statistically different from 1 (1 does not enter the confidence interval 0.9695–0.8857, taking into account the standard error of the regression coefficient). The same concerns the intercept (0 is not included in the confidence interval 0.0724 ± 0.042). Evidently this is due to the observed deviations of q-min and q-max mostly for weaker anisotropic BC-BS samples (Fig. 3(a)).

Table 2. (continued).

No		ANISOTROPY OF TRM1						ANISOTROPY OF TRM2				
material		440 (deg. C)		L	F	P		620 (deg. C)		L	F	P
		D	I	K1/K2	K2/K3	K1/K3		D	I	K1/K2	K2/K3	K1/K3
45-26P	K1	139	3	1.08	1.12	1.21	K1	326	1	1.06	1.10	1.17
tile	K2	35	77		T		K2	58	62		T	
in constr.	K3	230	12		0.21		K3	235	28		0.23	
34-1P	K1	298	14	1.04	1.14	1.18	K1	318	13	1.21	1.17	1.43
brick	K2	66	68		T		K2	90	71		T	
in constr.	K3	204	16		0.57		K3	225	14		-0.09	
34-12P	K1	21	2	1.02	1.36	1.40	K1	229	5	1.10	1.56	1.72
brick	K2	290	12		T		K2	320	12		T	
in constr.	K3	121	78		0.86		K3	119	77		0.65	
34-15P	K1	321	11	1.43	1.07	1.53	K1	327	12	1.46	1.08	1.46
brick	K2	194	73		T		K2	234	14		T	
in constr.	K3	54	13		-0.66		K3	96	71		0.74	
34-16P	K1	242	0	1.24	1.20	1.50	K1	42	8	1.23	1.18	1.46
brick	K2	332	53		T		K2	305	41		T	
in constr.	K3	152	37		-0.08		K3	141	47		-0.11	

The shape parameter T for different temperatures and different kinds of samples is given in Fig. 4. Obviously, the oblate form of anisotropy ellipsoids prevails for all kind of samples and for the two evaluations. This is linked with the shape-related magnetic fabric for bricks and tiles and with the mechanically produced one for baked clay ovens' floors. The similarity in the TRM anisotropy evaluated at two temperatures is even better revealed in case of pottery having the highly expressed 'easy plane' of magnetization (Genevey *et al.*, 2003).

3.2 Comparison of TRM and IRM anisotropy parameters

The IRM anisotropy evaluation of the 24 prehistoric samples was carried out in the Sofia laboratory after the Thellier experiment had been performed in the Rennes laboratory. The IRM anisotropy determination for the other 32 samples of different type and age was also carried out in the Rennes laboratory after the Thellier experiment. The only difference is that the residuals are measured after the subsequent three-axis AF static demagnetization in Rennes. There are 29 BR-TL samples for which the IRM anisotropy had not been determined. We will therefore compare IRM and TRM anisotropy tensors for 56 samples altogether.

We have shown that, in the case of TRM tensors obtained for two temperatures, the directions of the principal axes do not coincide very well in case of lower anisotropy of baked clay plasters and burnt soils. Because of this weak anisotropy and related large confidence angles (see Fig. 2(b)), mutual permutation of the principal axes is possible. This may be a reason for the moderate correlation that was obtained between anisotropy parameters of IRM and TRM1 or TRM2 tensors (Fig. 5(a, c)). The expected linear dependence between P(IRM) and P(TRM) is badly expressed ($r^2 = 0.21$ for Fig. 5(a) and $r^2 = 0.4$ for Fig. 5(c)) for the two temperatures, with a slight amelioration when a better holder was used for the TRM2 anisotropy measurements. Without always being the case, the remanence fabric in the studied collection of archaeological materials points to prevailed flattening for both BC-BS and BR-TL (Fig. 5(b, d)).

The normalized principal values of the IRM (r_i) and TRM (q_i) ellipsoids (the normalization also made by their average) for all studied samples show a good linear relationship for each of the two TRM1 (Fig. 6(a)) and TRM2 (Fig. 7(a)) anisotropy evaluations. Such a relationship can be considered to be a precondition for a similar shape of both tensors, as shown by Stephenson *et al.* (1986) when the regression line passes through the origin of the coordinate system. The linear relationship between r_i and q_i in our case deviates from the expected slope (not crossing the origin), which points to different shapes of the two ellipsoids (Figs. 6(a) and 7(a)). If we consider the same relationship separately for BC-BS and for BR-TL, we come to an interesting conclusion (Figs. 6(b, c) and 7(b, c)). It appears that the regression line of normalized principal values of BC-BS samples obtained for the two temperatures (Figs. 6(b) and 7(b)) deviates negligibly from the origin of the coordinate system (statistically, 1 and 0 enter the confidence intervals of the regression coefficient and of the intercept), suggesting the similarity of the two ellipsoid shapes. In this case, we have a confirmation of the Stephenson *et al.* (1986) assumption for the equality of TRM and IRM anisotropy ellipsoids shapes made in these authors' paper on the basis of only five samples. The increase in the correlation coefficient for BC-BS at the second anisotropy evaluation (TRM2; Fig. 7(b)) reflects the usage of better sample holders in this case. The regression line between the r_i and q_i obtained from BR-TL samples (Figs. 6(c) and 7(c)) with a good correlation coefficient ($R^2 = 0.85$ and $R^2 = 0.83$) deviates substantially from the origin of the coordinate system. This observation indicates that our results obtained from bricks/tile samples do not confirm the equality of the TRM and IRM ellipsoid shapes.

4. Anisotropy Effect on the Palaeointensity Evaluations

In further studies we used the TRM1 anisotropy parameters obtained at intermediate temperatures of 428, 440, or

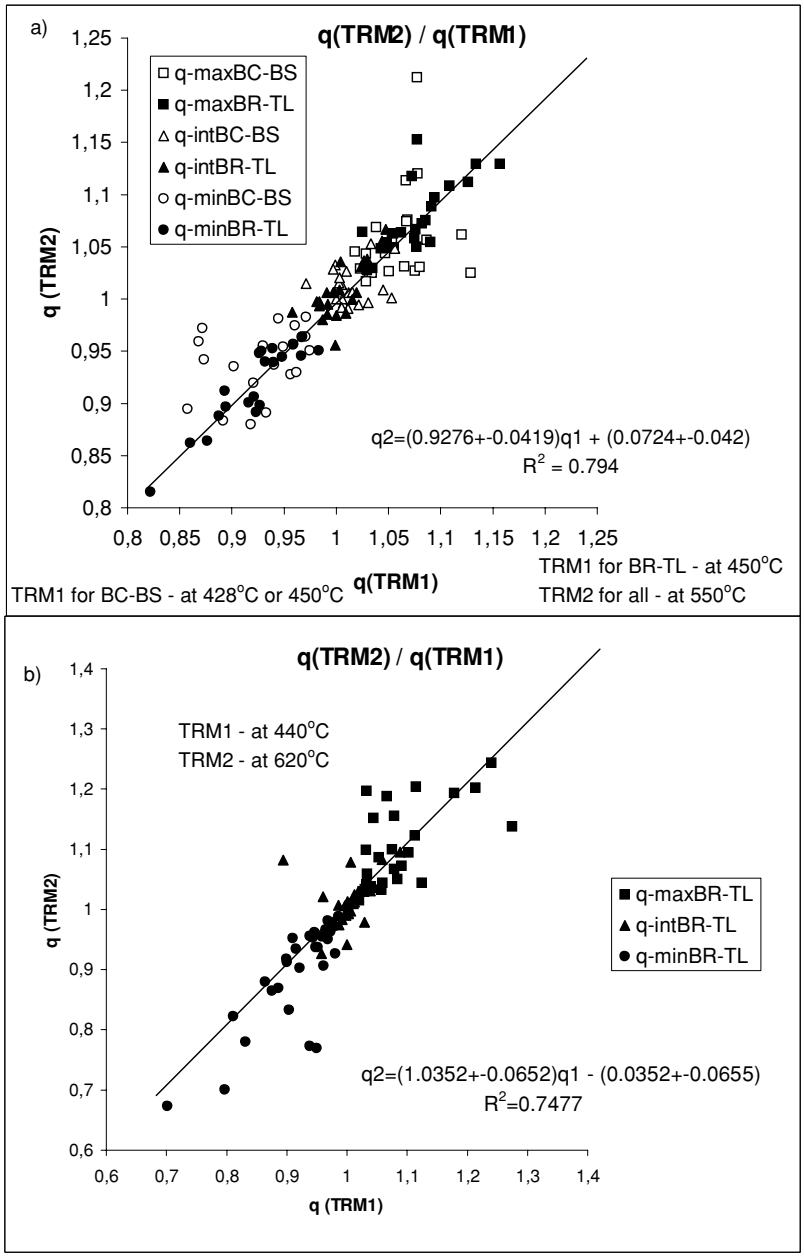

Fig. 3. Relationship between normalized principal values of the TRM1($q1$) and TRM2($q2$) ellipsoids measured at two temperatures ($q_x = \mathrm{TRM}_{xx}/((\mathrm{TRM}_{xx} + \mathrm{TRM}_{yy} + \mathrm{TRM}_{zz})/3)$ etc.) for the studied samples: (a) results from several experimental series for palaeointensity determination are combined; (b) results from a large BR-TL series for palaeointensity determination with two TRM anisotropy evaluations using a holder permitting good positioning of the samples. Temperature levels are given correspondingly. The best fitted straight lines are given with their errors.

450°C, paying particular attention to the identical shapes of the anisotropy ellipsoids obtained by the evaluations at two temperatures (Fig. 3(b)). Moreover and very important, these steps were included in the temperature interval for the palaeointensity determinations when the experimental points of 550° or 620°C at which the TRM2 anisotropy had been evaluated were only rarely taken for calculation of palaeointensity results. Some examples are given in Fig. 8.

The degree of anisotropy P(TRM), P(IRM) and the correction factors f determined on each sample, using both TRM and IRM tensors and the direction of NRM, in sample co-ordinates, are shown in Table 3. In this table, the obtained correction factor f_{IRM} for BR-TL, using the IRM anisotropy ellipsoid, are given in italics, and they are not taken for further considerations. The histogram of correction factors f obtained through TRM and IRM anisotropy determinations are shown in Fig. 9(a) only for samples of BC-BS for which we proved that the IRM ellipsoid can be used instead of the TRM one. The correction factor obtained through TRM anisotropy ellipsoid for all studied samples is given in Fig. 9(b). The correction factor is typically lower than 5%. This is an unexpected result, especially for the brick's samples, which have a quite strong remanence anisotropy (Fig. 1).

According to Aitken *et al.* (1981) and Odah *et al.* (2001), the most important factor for the bias from the true palaeointensity is the angle between the NRM, carried by samples, and the imposed laboratory field. In our Thel-

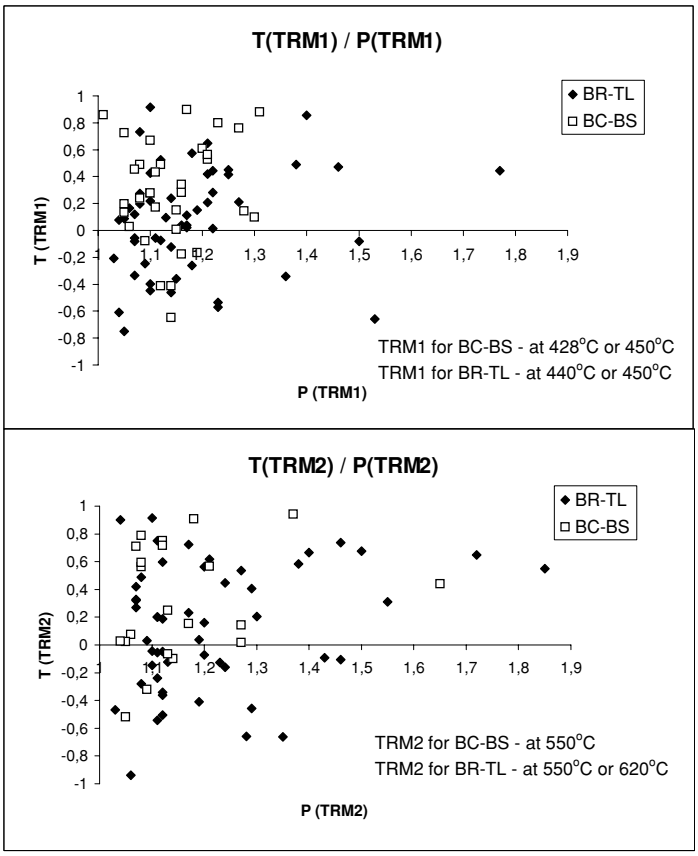

Fig. 4. Shape anisotropy parameter T versus degree of anisotropy P for baked clay/burnt soil (BC-BS) and for bricks/tiles (BR-TL) at the different temperatures shown in each graph.

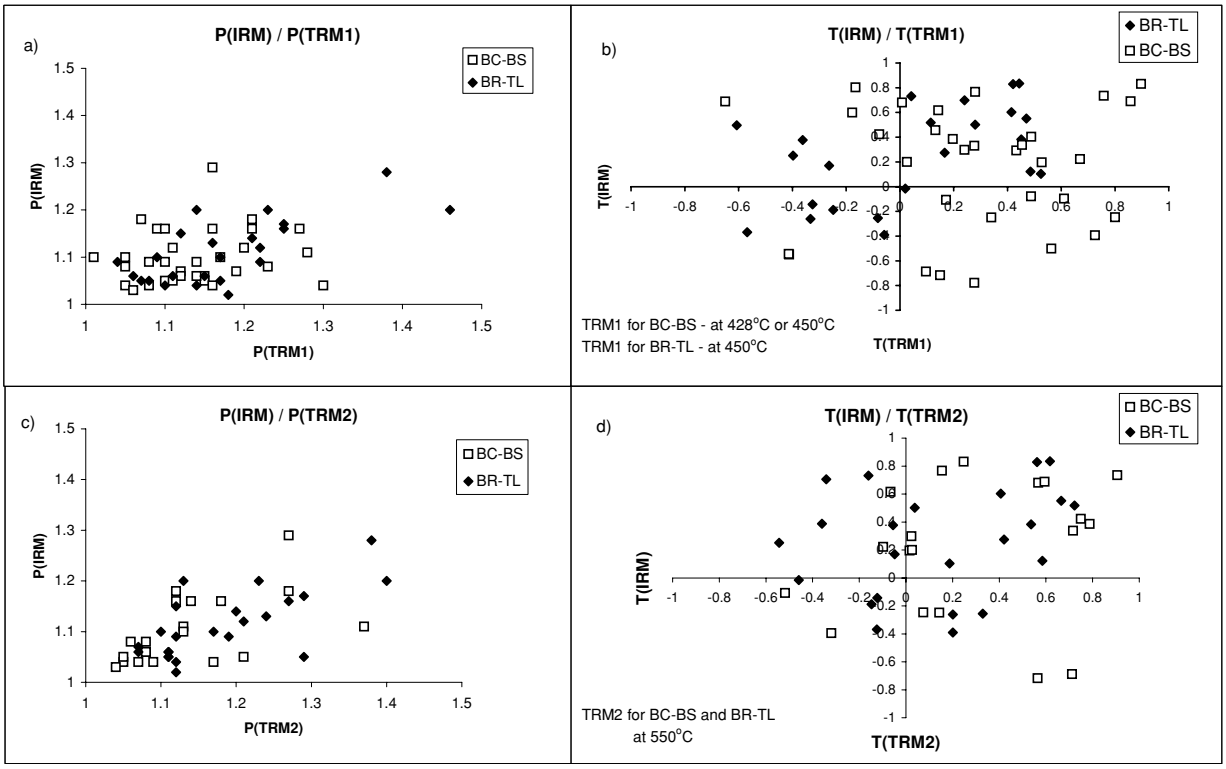

Fig. 5. Different relationships between degrees of anisotropy and shape parameters as obtained by IRM and TRM ellipsoids.

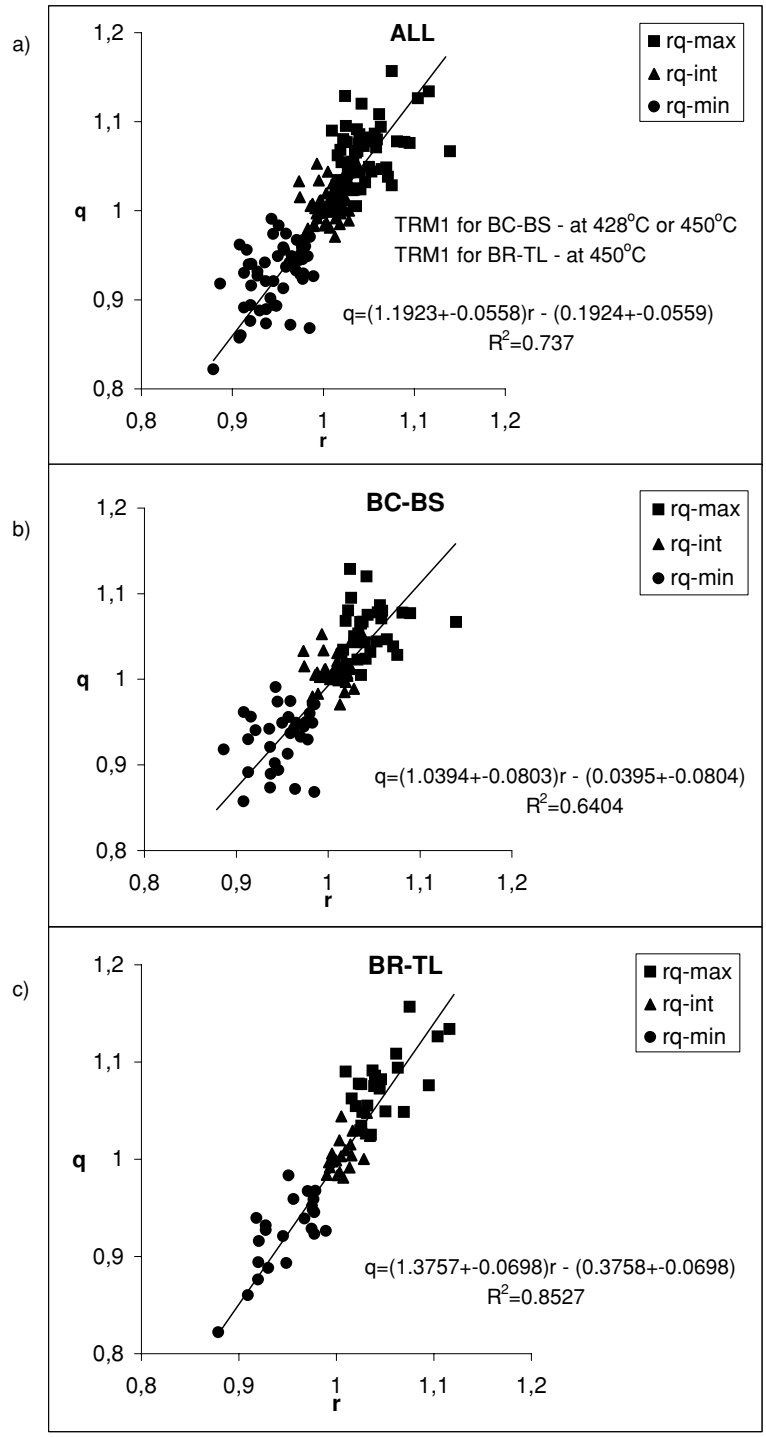

Fig. 6. Comparison of normalized principal axes' values of the IRM ($r_x = \mathrm{IRM}_{xx}/((\mathrm{IRM}_{xx} + \mathrm{IRM}_{yy} + \mathrm{IRM}_{zz})/3)$ etc.) and TRM ($q_x = \mathrm{TRM}_{xx}/((\mathrm{TRM}_{xx} + \mathrm{TRM}_{yy} + \mathrm{TRM}_{zz})/3)$ etc.) ellipsoids at lower temperature (TRM1) level, as noted in: (a) all; (b) and (c) separately for different types of materials. The best fitted straight lines are given with their errors. The temperatures of TRM1 anisotropy evaluations for different experimental series are given as a legend in Fig. 6(a).

lier's experiment, the laboratory field is applied along the Z axes of the samples (that is $I_{\mathrm{lab}} = 90^{\circ}$). Knowing that the direction of H_{lab} is along the Z axis, we define the angle $(90 - I_{\mathrm{NRM}})$ as the angular discrepancy between H_{lab} and the carried NRM. We define the angle α as the angle between the direction of the maximum principal axis of the TRM anisotropy ellipsoid (given in Tables 1 and 2) and the NRM direction (given in Table 3). Finally, we define the correction, due to the magnetic anisotropy, as $|1 - f|$.

Data reported in Fig. 10(a) indicate that the values of the correction factors do not depend on the angles between the NRM directions and the direction of maximum axes of the TRM anisotropy ellipsoids. This lack of systematic dependence on α is supported by the random directions of the K_{max} (TRM) for a given structure, reported recently by Gomez-Paccard *et al.* (2006) based on their study of baked clay materials from pottery kilns. The same is also evident from the 3D-plot in Fig. 10(b), where the parameter

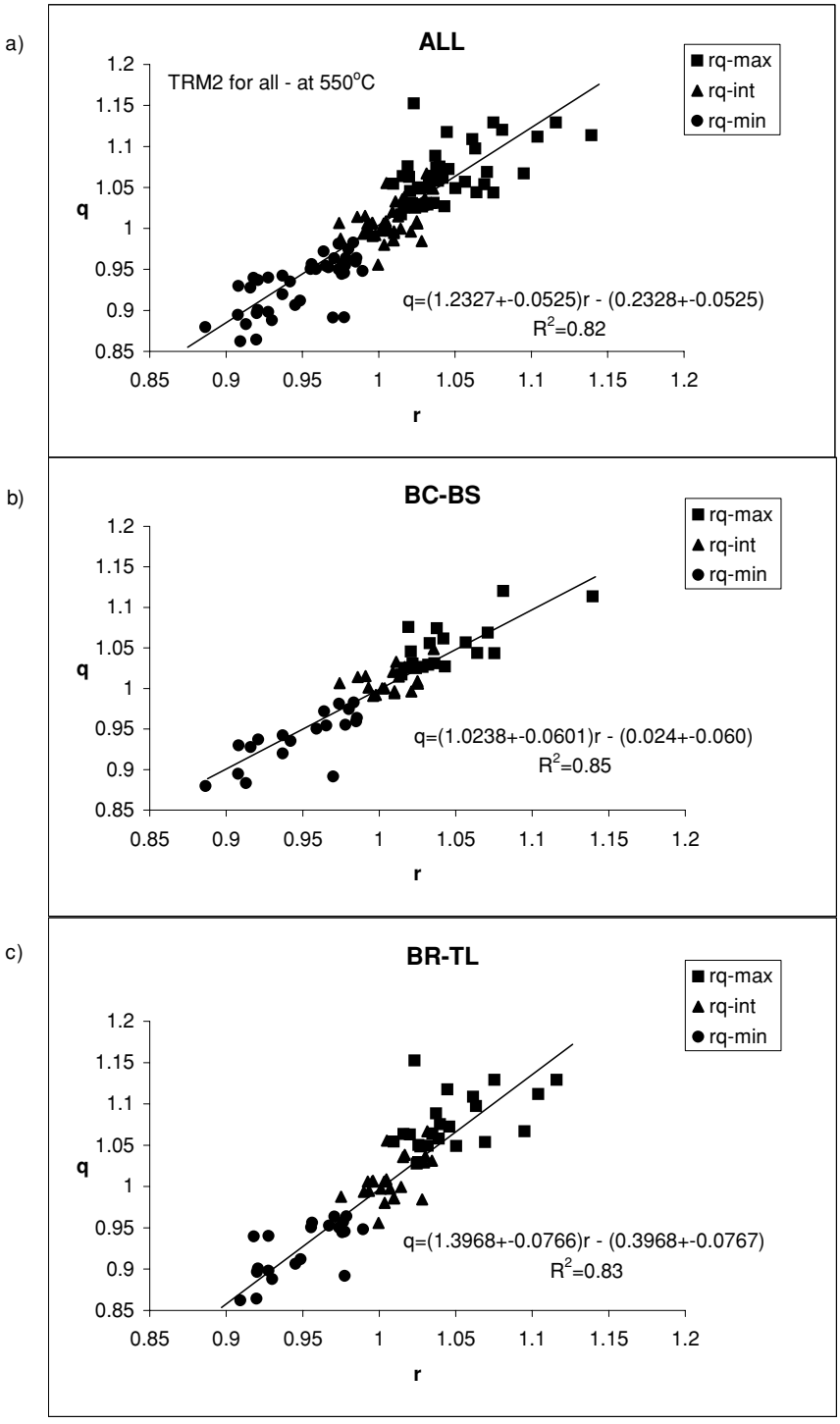

Fig. 7. As in Fig. 6 but for the higher temperature of 550°C.

P (degree of TRM anisotropy) is included as well. In the collection studied here, there are few cases of high P, which probably makes the upper part of the surface plot less well defined, but the trend is evident. In Fig. 11, a contour-plot of the TRM anisotropy degree P, angular discrepancy between $H_{\rm lab}$, and the carried NRM $(90 - I_{\rm NRM})$, and the correction factor $|1 - f|$ for all the samples is presented. The map is drawn using Kriging as an interpolation method. It appears that the correction factor $|1 - f|$ increases with P and $(90 - I_{\rm NRM})$.

In order to estimate the general relation between the two factors $(90 - I_{\rm NRM})$ and P on the one hand and the obtained correction parameter f (through $|1 - f|$) on the other, the equation of the plane obtained by a polynomial regression of the 83 points was determined. The plane is defined as: $Z(X, Y) = A_{00} + A_{01}Y + A_{10}X$ with $A_{00} = -0.1239$; $A_{01} = 0.1229$; $A_{10} = 0.0100$, where A_{01} is the coefficient for the degree of anisotropy and A_{10} is the coefficient for the angular discrepancy between $H_{\rm lab}$ and the carried NRM $(90 - I_{\rm NRM})$. In order to verify the relation, the isotropic case with $Y = 1$ (i.e., $P = 1.00$) and $X = 0$ (i.e., $(90 - I_{\rm NRM}) = 0$) is considered. Thus, $Z(0, 1) = 0.001$, which

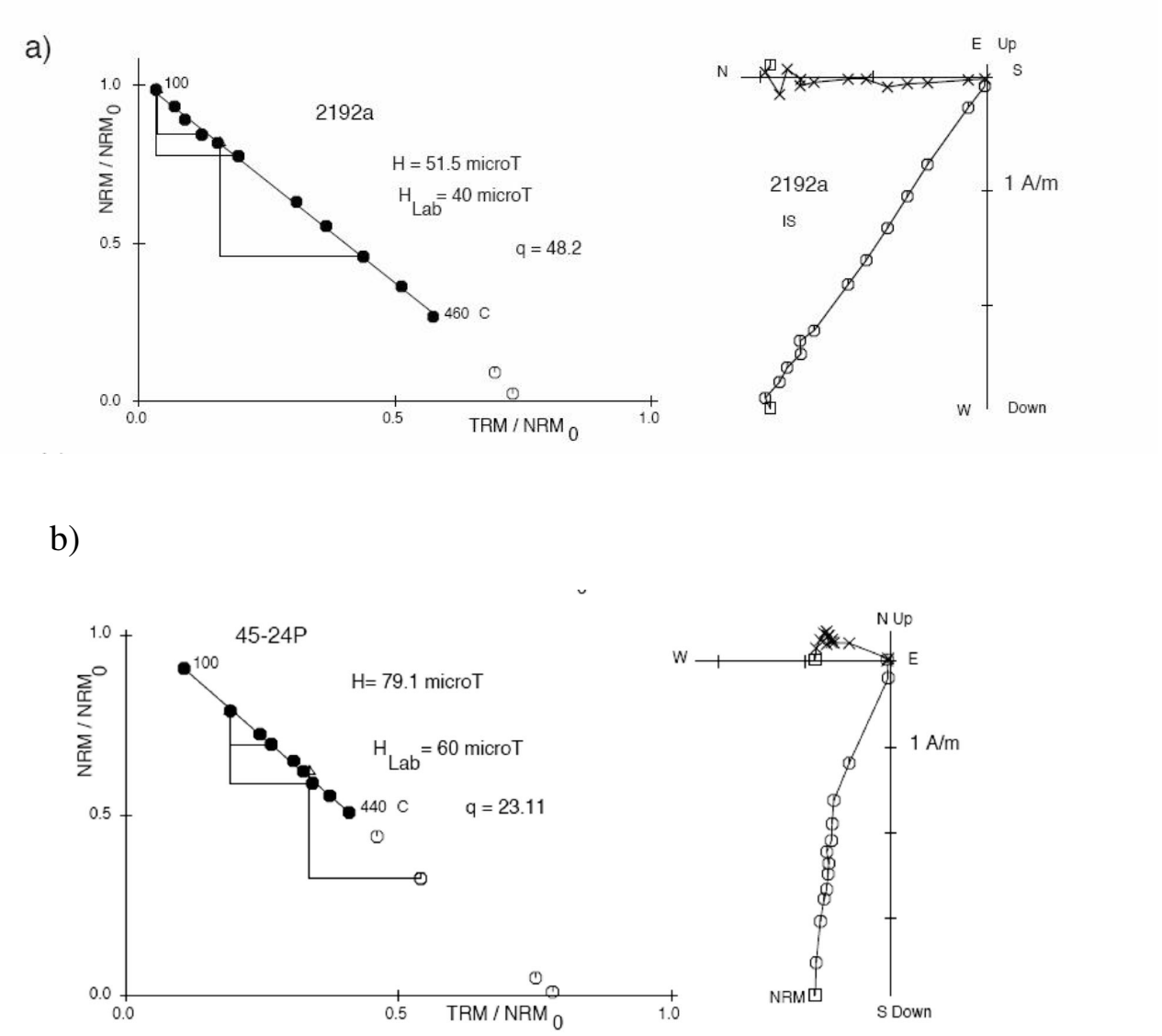

Fig. 8. Palaeointensity results of 2192a (BC-BS sample) and 45-24P (BR-TL sample) with the pTRM tests and Zijderveld diagrams. Points represented as solid circles are taken into the calculation of the regression line. The two-component remanence carried by the 45-24P tile in the kiln's construction is evident. The results shown are before anisotropy correction (Table 3). It is evident that the TRM1 evaluation is made in the temperature interval chosen for the palaeointensity determination.

clearly satisfies the physical meaning.

It is clear that the degree of anisotropy P has the biggest impact on the correction factor, but the influence of the angular discrepancy between $H_{\rm lab}$ and the carried NRM expressed by $(90 - I_{\rm NRM})$ cannot be neglected. Unfortunately, the programme used for the polynomial regression equation does not give us the standard errors of the calculated coefficients, and we cannot examine their statistical significance at this stage of study.

Figure 11 reveals that five points (marked with their α values) do not follow the general trend. A new calculation excluding these points leads to very similar coefficients, which are insignificantly different from the values calculated above. We conclude that these points have no important influence upon the trend observed between the parameters P and $(90 - I_{\rm NRM})$, and the correcting factor.

However, it has been mentioned above that the upper part of the surface plot (Fig. 10(b)) is less well defined because of the low density of data with higher values of P. To estimate this ambiguity, we have recalculated the polynomial regression, excluding P data higher than 1.3. The obtained new values of the regression coefficients using the remaining 75 points are as follows: $A_{00} = -0.1540$; $A_{01} = 0.1494$; $A_{10} = 0.0114$. Thus, the relation between them remains the same. The value of the regression coefficient A_{01} (related to P) is again one order higher than that of the regression coefficient A_{10} (related to the angular difference between the field directions of the NRM and those of the laboratory). This is a strong argument in support of the above-stated vision on the highest influence of P values upon the anisotropy correction of the palaeointensity evaluations.

5. Discussion

Genevey and Gallet (2002) and Bowles *et al.* (2002) have recently reported that the TRM anisotropy effect on the

Table 3. The effect of anisotropy correction on the obtained palaeointensity results (second, third and fourth columns). The age and the type of used material are specified in the last column. Temperat. Int. (deg) = temperature interval in degrees Celsius used to calculate the palaeointensity; Fa non-corr. = palaeointensity before correction; Fa corr. = palaeointensity after correction of anisotropy. When the average intensity per site is calculated, it is given with its dispersion. The change in the inter-sample dispersion in percentage is given below that corrected for the anisotropy site's palaeointensity. Remanence anisotropy parameters determined for the TRM and IRM tensors are shown in the fifth to eighth columns. P(TRM) = degree of TRM anisotropy; D (deg), I (deg) (TRM) = declination (inclination) of the maximum axis of the TRM ellipsoid, in sample co-ordinates; P(IRM) = degree of IRM anisotropy. The ninth and tenth columns show the correction factors f, determined through the TRM (f (TRM)) and IRM (f (IRM)) tensors, respectively. The direction of the carried NRM vector is given in the eleventh and twelfth columns; I (deg) and D (deg) = inclination and declination of the NRM, respectively, in sample co-ordinates.

	THELLIER EXPERIMENT			REMANENCE ANISOTROPY						NRM		AGE
No	Temperat. int. (deg)	Fa non-cor. (microT)	Fa cor. (microT)	Kmax/Kmin P(TRM1)	Kmax (TRM) D (deg)	I (deg)	Kmax/Kmin P(IRM)	f (TRM1)	f (IRM)	I (deg)	D (deg)	MATERIAL
2192a	100-460	51.48	51.64	1.11	31	60	1.12	1.00	1.06	55	359	13 c. AD
2192b	180-430	57.25	57.97	1.20	351	75	1.12	1.01	0.98	60	7	baked clay
2168a	100-500	58.51	61.37	1.17	108	32	1.10	1.05	1.05	58	18	11 c. AD burnt soil
2215b	100-500	51.74	51.64	1.01	218	0	1.10	1.00	1.03	61	13	11-12 c. AD baked clay
2221b	220-500	58.83	59.27	1.12	237	44	1.06	1.01	1.00	68	340	9 c. AD
2223b	190-550	66.2	67.28	1.16	115	25	1.04	1.02	1.00	64	346	baked clay
2073a	100-550	69.43	66.35	1.30	261	43	1.04	0.96	1.00	61	332	ca 4 c. BC burnt soil
2085v	100-500	86.65	93.33	1.28	79	51	1.11	1.08	1.05	58	340	ca 4 c. BC
2085g	100-460	89.32	96.61	1.16	112	64	1.16	1.08	1.06	56	340	burnt soil
2241a	100-500	69.33	67.56	1.09	173	1	1.16	0.97	0.96	56	353	ca 4 c. BC
2242a	235-428	62.68	65.01	1.21	54	22	1.16	1.04	0.98	50	260?	burnt soil
2253a	100-550	78.45	75.32	1.10	131	3	1.09	0.96	0.95	46	345	ca 4 c. BC
2264v	paleoint.	result	discarded	1.21	241	24	1.18	1.03	0.96	61	342	burnt soil
I 9v	100-398	44.59	45.84	1.10	238	46	1.05	1.03	1.02	59	342	ca 4 c. BC?
I 11b	100-398	38.85	39.46	1.15	260	44	1.06	1.02	1.02	66	5	baked clay
CA54a	100-460	44.53	39.88	1.31	156	2	1.11	0.90	1.02	45	342	Bronze baked clay
D174g	100-398	47.59	47.68	1.15	152	19	1.05	1.00	1.03	57	355	Bronze
D192v	180-430	47.2	46.02	1.08	65	14	1.09	0.98	0.97	54	354	baked clay
GV33b	100-430	61.1	60.88	1.05	179	0	1.10	1.00	1.02	62	350	Bronze
GV45v	100-460	60.02	61.86	1.23	124	40	1.08	1.03	1.02	57	352	baked clay
2145b	100-550	63.36	68.59	1.19	126	44	1.07	1.08	0.99	65	309	Iron burnt soil
86v	230-540	65.72	65.71	1.06	101	4	1.03	1.00	0.99	62	3	end 6 c. AD baked clay
DG37d	100-460	63.41	62.43	1.14	140	19	1.09	0.98	1.03	65	183	ca 4c.BC?
DG45d	paleoint.	result	discarded	1.12	110	28	1.07	0.99	1.01	72	356	baked clay
DG23e	paleoint.	result	discarded	1.05	212	13	1.08	1.00	1.00	70	329	
94b	230-540	72.3	72.23	1.14	175	1	1.06	1.00	1.01	78	330	10 c. AD baked clay
101v	190-540	79.34	79.34	1.08	57	29	1.04	1.00	1.00	74	20	10 c. AD baked clay

Table 3. (continued).

No	THELLIER EXPERIMENT			REMANENCE ANISOTROPY						NRM		AGE
	Temperat. int. (deg)	Fa non-cor. (microT)	Fa cor. (microT)	Kmax/Kmin P(TRM1)	Kmax (TRM) D (deg)	I (deg)	Kmax/Kmin P(IRM)	f (TRM1)	f (IRM)	I (deg)	D (deg)	MATERIAL
641a	190-550	83.66	83.94	1.11	81	39	1.05	1.00	1.00	72	338	641-
642b	190-540	73.62	72.67	1.07	44	8	1.18	0.99	0.98	71	342	647 AD
1576a	190-540	83.01	82.3	1.16	53	45	1.29	0.99	1.02	67	143	burnt soil
	average	80.1+-5.62	79.64+-6.09									
			-8%									
1788a	190-450	68.5	65.89	1.27	100	1	1.16	0.96	0.97	67	17	10 c. AD
												baked clay
1509a	paleoint.	result	discarded	1.05	267	9	1.08	1.03	1.01	-40	357	7 c. AD
												burnt soil
69b	190-420	56.24	56.51	1.08	353	46	1.05	1.01	*1.00*	57	59	5-6 c. AD
70b	190-450	61.26	59.08	1.09	198	10	1.10	0.96	*0.97*	-52	39	bricks
268a	190-550	65.65	62.65	1.25	170	1	1.16	0.95	*0.97*	-24	175	5-6 c. AD
269a	190-450	57.98	60.98	1.38	171	50	1.28	1.05	*1.13*	-5	160	bricks
270a	230-540	55.93	58.65	1.22	188	7	1.12	1.05	*1.04*	67	300	
	average	59.85+-5.1	60.76+-2.01									
			61%									
302v	190-450	67.82	65.59	1.25	6	9	1.17	0.97	*0.97*	58	340	6 c. AD
305a	230-450	58.36	59.53	1.46	353	3	1.20	1.02	*1.01*	65	315	bricks
376b	190-450	58.17	57.21	1.21	170	2	1.14	0.98	*1.02*	24	107	6 c. AD
379a	190-420	59.78	60.33	1.06	285	60	1.06	1.01	*1.01*	12	340	bricks
551b	190-450	63.29	62.62	1.07	39	2	1.07	0.99	*0.99*	60	359	6 c. AD
552a	100-400	69.84	69.97	1.08	40	16		1.00				bricks in
1609a	paleoint.	result	discarded	1.14	112	40	1.21	1.03	*1.1*	34	26	6 c. AD
1596v	100-510	56.67	62.62	1.77	193	65		1.11		-15	5.4	bricks
B175b	100-440	59.06	60	1.03	207	50		1.02		14	330	5 c. AD
B178a	200-440	55.5	55.33	1.13	193	29		1.00		-53	280	bricks
B182b	100-510	61.8	66.6	1.12	184	62		1.08		-22	210	
	average	58.79+-3.16	60.64+-5.66									
			-36%									
B207b	150-360	73	69.1	1.07	153	20		0.95		-3	330	6 c. AD
B210a	100-360	57.42	58.65	1.07	248	58		1.02		60	120	bricks
B211a	100-480	62.82	62.3	1.04	329	3		0.99		60	298	
	average	64.41+-7.91	63.35+-5.3									
			33%									
36-3	paleoint.	result	discarded	1.11	274	68	1.06	1.00	*1.01*	73	5	7-8 c. AD
36-8	190-550	75.53	73.1	1.12	294	19	1.15	0.97	*0.99*	66	17	tiles in
36-13	190-550	79.38	74.79	1.17	14	29	1.10	0.94	*0.99*	64	2	kiln's
36-13a	100-480	83.82	78.91	1.17	210	24		0.94		-62	17	construction
36-16	190-550	75.64	74.91	1.17	222	9	1.05	0.99	*0.99*	68	10	
36-17	190-420	75.13	75.18	1.04	210	11	1.09	1.00	*1.01*	66	10	
36-19	190-550	73.97	73.57	1.10	162	9	1.05	0.99	*1.00*	70	13	
36-19a	240-510	81.95	81.82	1.10	322	45		1.00		-73	196	
	average	77.92+-3.82	76.04+-3.16									
			17%									

palaeointensity determinations from pottery lead to correction factors of up to 30%. This has been experimentally shown by Odah *et al*. (2001) for pottery in which the easy plane seems to play the major role. Our results indicate that the effect of the anisotropy upon palaeointensity determinations is lower on BR-TL and lower still on BC-BS than on pottery, as mentioned in previous comparative studies on the basis of less numerous collections (Jordanova *et al*., 1995; Kovacheva *et al*., 1998). Furthermore, in an archaeomagnetic study of Danish materials from bricks, a few

Table 3. (continued).

No	THELLIER EXPERIMENT			REMANENCE ANISOTROPY						NRM		AGE
	Temperat. int. (deg)	Fa non-cor. (microT)	Fa cor. (microT)	Kmax/Kmin P(TRM1)	Kmax (TRM) D (deg)	I (deg)	Kmax/Kmin P(IRM)	f (TRM1)	f (IRM)	I (deg)	D (deg)	MATERIAL
41-1	190-450	92	90.13	1.23	48	10	1.20	0.98	*0.93*	63	13	6-7 c. AD
41-4	190-490	129.21*	126.63*	1.16	52	12	1.13	0.98	*0.99*	65	14	tiles in
41-6	paleoint.	result	discarded	1.14	53	2	1.04	1.01	*0.99*	68	4	kiln's
41-6a	240-480	100.43	99	1.08	86	11		0.99		-67	41	construction
41-8	230-420	99.35	100.35	1.18	225	16	1.02	1.01	*1.00*	73	15	
41-8a	20-480	108.88	109.97	1.18	48	3		1.01		-70	0	
41-9	190-550	99.98	97.1	1.22	157	0	1.09	0.97	*0.98*	68	9	
41-19	paleoint.	result	discarded	1.15	25	30	1.06	0.97	*0.99*	66	4	
41-19a	300-480	79.57*	79*	1.07	215	8		0.99		-66	140	
	average	100.04+-5.99	99.31+-7.14									
			-16%									
45-8P	20-510	78.95	81.41	1.10	87	12		1.03		55	194	6-7 c. AD
45-12P	100-300	78.18	79.33	1.14	40	2		1.01		85	220	tiles in
45-15P	paleoint.	result	discarded	1.19	33	4						kiln's
45-16P	paleoint.	result	discarded	1.23	217	42						construction
45-17P	100-510	82.95	81.52	1.22	126	2		0.98		67	208	
45-18P	100-510	84.55	84.38	1.21	131	40		1.00		69	197	
45-19P	150-510	69.98*	69.36*	1.05	112	7		0.99		73	203	
45-20P	100-560	82.38	82.02	1.05	158	9		1.00		71	196	
45-21P	150-360	73.65	77	1.27	115	21		1.04		70	178	
45-22P	100-440	83.63	84.07	1.17	300	11		1.01		75	220	
45-23P	100-510	86.42	86.44	1.10	26	21		1.00		69	220	
45-24P	100-440	79.06	78.75	1.10	136	12		1.00		72	286	
45-25P	100-560	81.11	80.65	1.36	43	5		0.99		74	206	
45-26P	100-560	79	80.41	1.21	139	3		1.02		73	197	
	average	81.07+-3.58	81.45+-2.72									
			24%									
34-1P	100-560	74.75	73.92	1.18	298	14		0.99		55	90	4-5 c. AD
34-12P	100-400	72.85	70.82	1.40	21	2		0.97		-47	330	bricks in
34-15P	100-620	80.41	72.86	1.53	321	11		0.91		49	348	kiln's
34-16P	100-440	69.55	65.35	1.50	242	0		0.94		56	358	construction
	average	74.39+-4.55	70.74+-3.82									
			16%									

ceramics, and burned clay from furnaces, Gram-Jensen *et al*. (2000) proved the negligible influence of the remanence anisotropy estimated by TRM anisotropy tensor, as has been done in the present study. In a more recent paper, Genevey *et al*. (2003) estimated the TRM anisotropy correction on the palaeointensity from both pottery and bricks from Syria. The obtained correction factor for bricks was found to cluster between 0.98 and 1.02 for 70% of the specimens, which is in excellent agreement with the results shown in this study. However, Leino and Pesonen (1994) reported stronger remanence anisotropy in bricks than in potsherds, but their conclusion was drawn on a very small number of experiments.

In a palaeointensity study on older potsherds from Ontario, Yu and Dunlop (2000) concluded that there is no correlation between the degree of remanence anisotropy and the estimated palaeointensity value. However, in our study, we were able to show that the values of the correcting factor of palaeointensity determinations, even if is low, depend on the degree of remanent anisotropy and also on the angle between the NRM direction and the laboratory field direction. In the recently developed new three-axis magnetometer (Le Goff and Gallet, 2004), the correction for anisotropy effect is automatically done by keeping the angle between the NRM and laboratory field direction less than 4°. This recent technological development will be a valuable tool and add precision to the obtained palaeointensity results from the most anisotropic objects such as pottery fragments (Rogers *et al*., 1979; Aitken *et al*., 1981; Jordanova *et al*., 1995). Our study has shown that when a difference between the applied laboratory field and that carried by the sample NRM exists, which is always the case in practice, the degree of anisotropy also plays an important role. As it can be seen in Table 3, the angle between the I_{NRM} and the laboratory field is not very large in most cases. Thus, despite a high degree of remanence anisotropy ($K_{\max}/K_{\min}$), the obtained correction factor f_{TRM} is not high (Table 3: samples GV45v; 94b; 1576a; 302a; 305a; 41-1; 41-9; 45-17P, 18P, 21P, 25P). However, large correction factors f_{TRM} are observed on a few samples which have a strong magnetic anisotropy and which carry a NRM in a direction that is far from the laboratory field direction (Table 3: samples CA54a; 269a; 1596v; B182b; 34-15P). The opposite is true in cases when the NRM direction is entirely different from

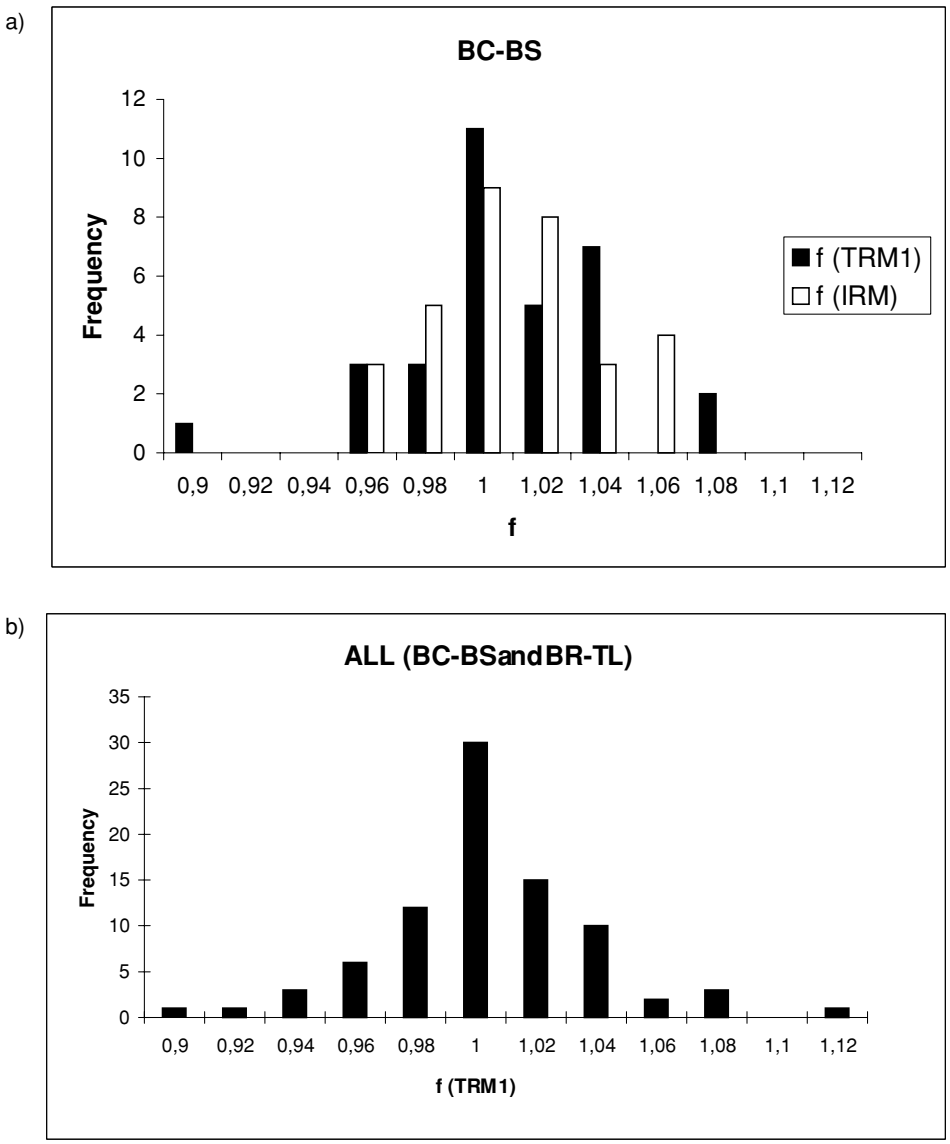

Fig. 9. (a) Histogram of frequency distribution of the obtained values of correction factor f determined through the anisotropy estimation of TRM and IRM tensors for BC-BS; (b) frequency distribution of the obtained values of correction factor f determined through TRM tensor at the intermediate (first) temperature for all studied samples.

the laboratory field but the degree of remanence anisotropy remains low; the correction factor is also not significant (Table 3: samples 1509a; 379a; B175b).

In Table 3, the average values of palaeointensity per sites, before and after the correction of anisotropy, are also reported when more than two samples were studied per site. In five of the seven cases of sites presented by BR-TL, the standard deviations around the means decrease after the corrections, although the average values themselves are not affected substantially. The change in the inter-sample dispersion after the anisotropy correction is given in percentage in the fourth column of Table 3, where the minus sign means a worsening of the dispersion. Looking closely at these figures, we can make a number of remarks. The BS samples of the first site have NRM directions (11th column) close to the direction of the laboratory field, and the anisotropy effect should be smaller, which is the case (-8%). The next site represented by bricks with a considerable degree of remanence anisotropy (fifth column) and two samples having NRM directions far away of the laboratory field direction shows the largest amelioration of the dispersion (61%). The two last sites presented in Table 3, having a substantial degree of TRM anisotropy, have different correction factors (ninth column), depending on the mutual orientation of NRM and laboratory field. In these two cases, the dispersion is also improved (24 and 16%), when sample 34-15P, with the highest P(TRM) and NRM's largest deviation from the laboratory field direction for these two sites, has the strongest correction factor. Thus, in order to obtain the best palaeointensity data on bricks and tiles, either a correction for anisotropy is needed or the laboratory field must be applied along the NRM direction. As far as baked clay plasters of ovens and kilns are concerned, we can trust the multiple published palaeointensity data without anisotropy correction, taking into account the results reported here. In fact, our results show that the anisotropy correction is small/insignificant for BC-BS materials and that these materials can be considered as isotropic. There re-

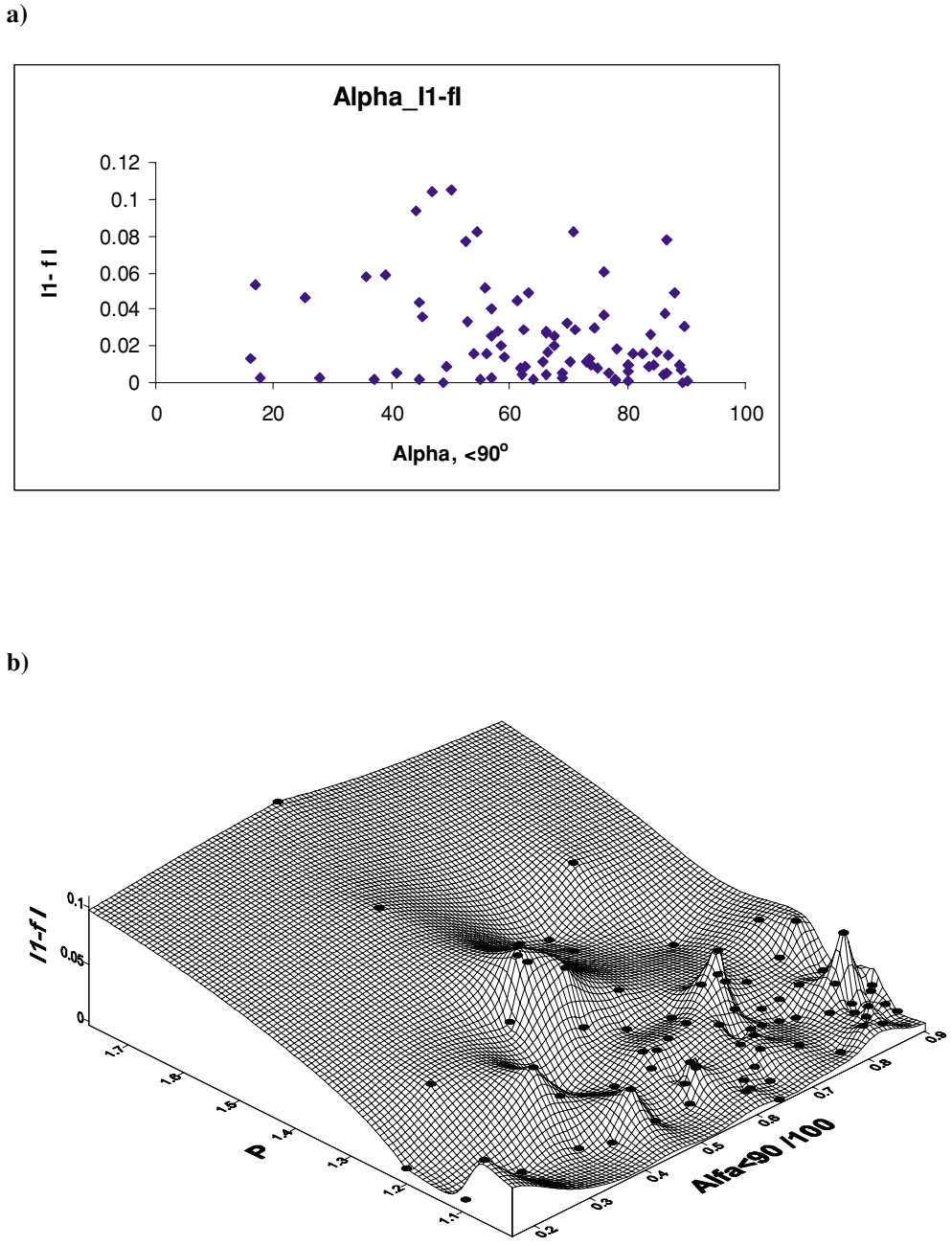

Fig. 10. (a) The anisotropy correction on the palaeointensity values as a function of the angle between NRM and the maximum axis of the TRM anisotropy ellipsoid (α); (b) 3-D plot representing the mutual influence of the degree of TRM anisotropy P and α on the correction of palaeointensity value $|1 - f|$. The values α on the X axis have been divided by 100 for better visualization.

sults, therefore, can be used in further compilation of worldwide palaeointensity data with an equal weight as that corrected for anisotropy results from, for example, potteries.

To avoid the unwanted multiple heating for TRM ellipsoid estimation, our results show that the laboratory-induced IRM remanence could be used instead when materials are baked clay/burnt soils. Only for this kind of material we have obtained a confirmation for the similarity of the anisotropy tensors shape of IRM and TRM remanence (Figs. 6(b) and 7(b)). In other words, replacing the TRM ellipsoid with the IRM one in the case of the BR-TL samples as a result of studied collection is not straightforward (Figs. 6(c) and 7(c)) despite the observed similarity of the principal axes directions in most of the cases. Hus *et al.* (2002), comparing the TRM and anhysteretic anisotropy ellipsoids (ARM) for bricks, come to the same conclusion, thereby confirming the similarity of the principal axes directions, but changes in the shape. They found an equality in ellipsoid shapes only between that of TRM and that of partial anhysteretic remanence (PARM).

6. Conclusions

1. The degree of remanence anisotropy of baked clay/burnt soil is significantly lower than that in bricks and tiles, which have shape anisotropy.
2. The comparison of remanence anisotropy at two temperature levels reveals that the tensor determination through measurements on three perpendicular direc-

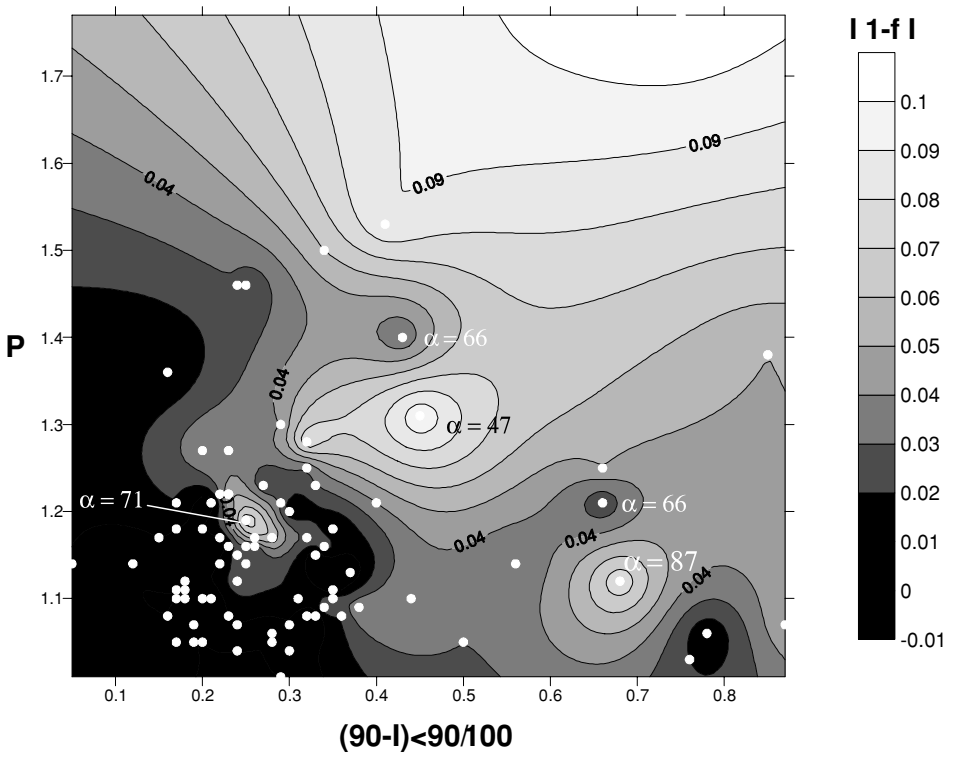

Fig. 11. Contour-plot representing the mutual influence of the degree of TRM anisotropy P and the bias of laboratory field from the direction of carried NRM: $(90 - I_{\mathrm{NRM}})$ on the anisotropy correction given as $|1 - f|$. As in Fig. 10, the values of $(90 - I_{\mathrm{NRM}})$ have been divided by 100 for better visualization.

tions, as done here, is probably not sufficiently precise for the determination of principal axes' directions, especially for samples with a weak anisotropy.

3. A small effect of the magnetic anisotropy on palaeointensity determinations for baked clay/burnt soils materials (BC-BS) is observed using either IRM or TRM tensors. The more time-consuming TRM tensor determination can be replaced by the IRM tensor of anisotropy for such material, which avoids possible mineralogical changes during heating.
4. The shape of the IRM anisotropy ellipsoid is not identical to that of the TRM anisotropy ellipsoid when bricks/tiles (BR-TL) are concerned and the IRM anisotropy cannot replace the TRM anisotropy evaluation for them.
5. The anisotropy correction of the palaeointensity results for the material different from pottery seems negligible (in the all studied samples but six, it is up to 6%); however, it improves the inter-samples dispersion for most of the sites studied here, as previously shown for similar materials (Chauvin *et al.*, 2000) and for palaeomagnetic samples with a strong petrofabric (Selkin *et al.*, 2000).
6. A detailed analysis of the influence of different parameters on the magnetic anisotropy correction on the palaeointensity values has shown that for the material used in this study, the correction is more sensitive to the degree of TRM anisotropy and to the angular distance between the laboratory field and NRM directions than to the angle between the NRM and the axis of maximum remanence anisotropy ellipsoid.

Acknowledgments. One of the authors (M.K.) expresses her gratitude to the Geosciences Laboratory (University of Rennes 1), where she has been granted leave to carry out 2 months of experimental work. The authors acknowledge their thanks to Dr. Lucien Daly from the IPGP laboratory in Saint-Maur for the useful discussions over the obtained results on the anisotropy. Special thanks are due to Dr. B. Henry for his comments on the initial version of the text and for his efforts and those of one anonymous reviewer on the thorough revision and valuable suggestions for the present manuscript. This helped considerably for further amelioration of the text and illustrations. Thanks are also due to the EPS journal's editor Dr. Masayuki Hyodo for his support and valuable advice during the long process of revisions and corrections. The experimental work was begun 1997 and has continued through the bilateral collaboration between DRI/CNRS-France and Bulgarian Academy of Sciences. The study has been partially supported by the AARCH EU contract No HPRN-CT-2002-00219 (Archaeomagnetic applications for the rescue of cultural heritage).

References

Aitken, M. J., P. A. Alcock, G. D. Bussel, and C. J. Shaw, Archaeomagnetic determination of the past geomagnetic intensity using ancient ceramics: allowance for anisotropy, *Archaeometry*, **23**(1), 53–64, 1981.

Bowles, J., J. Gee, J. Hildebrand, and L. Tauxe, Archaeomagnetic intensity results from California and Ecuador: evaluation of regional data, *Earth Planet. Sci. Lett.*, **203**, 967–981, 2002.

Carvallo, C. and D. J. Dunlop, Archeomagnetism of potsherds from Grand Banks, Ontario: a test of low paleointensities in Ontario around A.D. 1000, *Earth Planet. Sci. Lett.*, **186**, 437–450, 2001.

Coe, R. S., S. Gromme, and E. A. Mankinen, Geomagnetic paleointensities from radiocarbon-dated lava flows on Hawaii and the question of the Pacific nondipole low, *J. Geophys. Res.*, **83**, 1740–1756, 1978.

Chauvin, A., P. Y. Gillot, and N. Bonhommet, Palaeointensity of the Earth's magnetic Field, recorded by two Late Quaternary sequences at the Island of La Reunion (Indian Ocean), *J. Geophys. Res.*, **96**(B2), 1981–2006, 1991.

Chauvin, A., Y. Garcia, Ph. Lanos, and F. Laubenhaimer, Paleointensity of

the geomagnetic field recovered on archaeomagnetic sites from France, *Phys. Earth Planet. Inter.*, **120**, 111–136, 2000.

Daly, L. and H. Zinsser, Etude comparative des anisotropies de susceptibilite et d'aimentation remanente isotherme. Consequences pour l'analyse structurale et le paleomagnetisme, *Ann. Geophys.*, **29**, 189–200, 1973.

Garcia, Y., Variation de l'intensite du champ magnetique en France durant les deux derniers millenaires, PhD Thesis, University of Rennes 1, 1996.

Genevey, A. and Y. Gallet, Intensity of the geomagnetic field in Western Europe over the past 2000 years: New data from ancient French pottery, *J. Geophys. Res.*, **107**(B11), 2285, doi: 10.1029/2001 JB000701, 2002.

Genevey, A., Y. Gallet, and J.-Cl. Margeueron, Eigth thousand years of geomagnetic field intensity variations in the eastern Mediterranean, *J. Geophys. Res.*, **108**(B5), 2228, doi: 10.1029/2001 JB001612, 2003.

Gomez-Paccard, M., A. Chauvin, Ph. Lanos, J. Thiriot, and P. Jimenez-Castillo, Archeomagnetic study of seven contemporaneous kilns from Murcia (Spain), *Phys. Earth Planet. Inter.*, **157**, 16–32, doi:10.1016/j.pepi.2006.03.001, 2006.

Goulpeau, L., Ph. Lanos, and L. Langouet, The anisotropy as a disturbance of the archaeomagnetic dating method, in *Proc. 25th Int. Symposium of Archaeometry*, 54–58, Elsevier, 1989.

Gram-Jensen, M., N. Abrahamsen, and A. Chauvin, Archaeomagnetic Intensity in Denmark, *Phys. Chem. Earth (A)*, **25**(5), 525–531, 2000.

Henry, B., D. Jordanova, N. Jordanova, Ch. Souque, and Ph. Robion, Anisotropy of magnetic susceptibility of heated rocks, *Tectonophysics*, **366**, 241–258, 2003.

Hrouda, F., Magnetic anisotropy of rocks and its application in geology and geophysics, *Geophys. Surv.*, **5**, 37–82, 1982.

Hus, J., Anisotropy of TRM, in *Abstracts book of the 2nd meeting of AARCH (Archaeomagnetism Applied for Rescue Cultural Heritages)*, Leoben, September, 2001.

Hus, J., S. Ech-Chakrouni, and D. Jordanova, Origin of magnetic fabric in bricks: its implications in archaeomagnetism, *Phys. Chem. Earth*, **27**(25–31), 1319–1331, 2002.

Jelinek, V., Characterisation of the magnetic fabric of rocks, *Tectonophysics*, **79**, 63–67, 1981.

Jordanova, N., Rock magnetic studies in archaeomagnetism and their contribution to the problem of reliable determination of the ancient geomagnetic field intensity, PhD Thesis, Sofia, 1996 (in Bulgarian).

Jordanova, N., V. Karloukovski, and V. Spataras, Magnetic anisotropy studies on Greek pottery and bricks, *Bulg. Geophys. J.*, **21**(4), 49–58, 1995.

Jordanova, N., E. Petrovsky, and M. Kovacheva, Preliminary rock magnetic study of archaeomagnetic samples from Bulgarian prehistoric sites, *J. Geomag. Geoelectr.*, **49**, 543–566, 1997.

Jordanova, N., M. Kovacheva, I. Hedley, and M. Kostadinova, On the suitability of baked clay for archaeomagnetic studies as deduced from detailed rock-magnetic studies, *Geophys. J. Int.*, **153**, 146–158, 2003.

Kovacheva, M., N. Jordanova, and V. Karloukovski, Geomagnetic field variations as determined from Bulgarian Archaeomagnetic Data. Part II: The Last 8000 Years, *Surv. Geophys.*, **19**, 431–460, 1998.

Lanos, Ph., The effect of demagnetising field on thermoremanent magnetization acquired by parallel-sided baked clay blocks, *Geophys. J. R. Astron. Soc.*, **91**, 985–1012, 1987a.

Lanos, Ph., Archéomagnétisme des materiaux déplacés, applications à la datation des des matériaux de construction d'argile cuite en archéologie, Thèse de Doctorat, Université de Rennes 1, Rennes, 1987b.

Le Goff, M. and Y. Gallet, A new three-axis vibrating sample magnetometer for continuous high-temperature magnetization measurements: applications to paleo- and archeo-intensity determinations, *Earth Planet. Sci. Lett.*, **229**, 31–43, 2004.

Leino, M. A. H. and L. J. Pesonen, Archaeomagnetic intensity in Finland—the last 6400 years, Open File Report Q19/22.0/1994/1, 1994.

Marton, P., Archaeomagnetic directions: the Hungarian calibration curve, in *Palaeomagnetism and Tectonics of the Mediterranean Region*, edited by A. Morris and D. Tarling, 385–399, Geological Soc., Special Publication No 105, 1996.

Nagata, T., Y. Arai, and K. Momose, Secular variation of the Geomagnetic Total Force during the Last 5000 Years, *J. Geophys. Res.*, **68**(18), 5277–5281, 1963.

Odah, H., A. G. Hussain, V. Hoffmann, H. C. Soffel, M. El-Gamili, and H. Deebes, Effect of magnetic anisotropy on the experimentally determined palaeointensity of the geomagnetic field, *Earth Planets Space*, **53**, 363–371, 2001.

Rogers, J., J. M. W. Fox, and M. J. Aitken, Magnetic anisotropy in ancient pottery, *Nature*, **277**(5698), 644–646, 1979.

Selkin, P. A., J. S. Gee, L. Tauxe, W. P. Meurer, and A. J. Newell, The effect of remanence anisotropy on paleointensity estimates: a case from Archean Stillwater Complex, *Earth Planet. Sci. Lett.*, **183**, 403–416, 2000.

Stephenson, A., S. Sadikun, and D. K. Porter, A theoretical and experimental comparison of the anisotropies of magnetic susceptibility and remanence in rocks and minerals, *Geophys. J. R. Astron. Soc.*, **84**, 185–200, 1986.

Tarling, D. H. and F. Hrouda, *The magnetic anisotropy of Rocks*, Chapman and Hall, 1993.

Thellier, E. and O. Thellier, Sur l'intensite du shamp magnetique terrestre dans le passe historique et geologique, *Ann. Géophys.*, **15**, 285–376, 1959.

Veitch, R. J., I. G. Hedley, and J. J. Wagner, An investigation of the intensity of the geomagnetic field during roman times using magnetically anisotropic bricks and tiles, *Arch. Sci. Geneve*, **37**, Fasc. 3, 359–373, 1984.

Yang, S., J. Shaw, and T. Rolph, Archaeomagnetic studies of Peruvian pottery—from 1200 BC to 1800 AD, *J. Geomag. Geoelectr.*, **45**, 1193–1207, 1993a.

Yang, S., J. Shaw, and Q. Wei, A comparison of archaeointensity results from Chinese ceramics using Thellier's and Shaw's palaeointensity methods, *Geophys. J. Int.*, **113**, 499–508, 1993b.

Yu, Y. and D. Dunlop, Archaeomagnetism of Ontario potsherds from the last 2000 years, *J. Geophys. Res.*, **105**(B8), 19419–19433, 2000.

Yu, Y., D. Dunlop, L. Pavlish, and M. Cooper, Paleointensity determination on the Late Precambrian Tudor Gabbro, Ontario, *J. Geophys. Res.*, **106**(B11), 26331–26343, 2001.

M. Kovacheva (e-mail: marykov@abv.bg), A. Chauvin, N. Jordanova, P. Lanos, and V. Karloukovski